Trip 14:

Patagonia, Red Mountain, Hardshell

October, 1994

Bootprints Along the Cordillera

Porphyry Copper Deposits from Alaska to Chile

THIS PAGE

INTENTIONALLY BLANK

Dear Field Trip Participants:

On behalf of the **Arizona Geological Society, Society for Mining, Metallurgy and Exploration Inc., and the U. S. Geological Survey**, we bid you welcome to the Bootprints Along the Cordillera field trip program. We have assembled a collection of field trips that portray the geologic and mineralogic diversity that exists along the cordillera of North and South America.

We wish to thank all of the field trip leaders who volunteered their time, effort, and expertise to organize their individual trips. We also want to thank collectively, all of the mining companies and staff who graciously allowed us to visit their properties. Without their cooperation, this program would not have occurred. A special thanks goes to Kathie Harrigan of Asarco for her help in the compilation of the field trip guides. We also want to thank Tucson Blueprint who underwrote the complete reproduction cost of the guides.

Mark Miller and Jim Briscoe
Field Trip Co-Chairmen
October 2, 1994

THIS PAGE

INTENTIONALLY BLANK

To Field Trip Participants

This field trip is designed to give you an opportunity to examine the undisturbed, upper, near-paleosurface portion of porphyry copper alteration systems and compare the surface expression with drill hole data showing vertical zoning to potassic alteration and higher grade primary copper mineralization at depth. These "high-level" exposures of porphyry copper alteration-mineralization systems exhibit co-magmatic volcanic and sub-volcanic intrusive rocks and are characterized by widespread, abundant pyrite and a concentrically zoned pattern of metallization with metals occurring both in disseminated minerals and in exterior veins. The Hardshell silver deposit is part of the zoned sequence of metal deposits exterior to the Sunnyside center of alteration.

The field trip leaders, Fred Graybeal, Richard Ahern and Russell Corn were actively involved in the exploration programs at Red Mountain and Sunnyside since the inception of exploration in the early 1960's and have also participated in exploration of other "high-level" alteration systems. The Red Mountain and Hardshell portions of the trip will be a repeat of the 1981 and 1986 field trips. There has been little exploration activity since 1980 and no appreciable change to the geologic data and observations published in 1981. However, the geologic data on alteration and mineralization at Sunnyside have not been presented previously and are a welcome addition to our knowledge of the upper part of porphyry alteration systems.

I would like to express appreciation to James J. Quinlan, Fleetwood R. Koutz and Frederick T. Graybeal, the authors of material presented in this guidebook and to Richard Ahern, Fred Graybeal and others who volunteered as leaders and assisted with the field trip. I specifically wish to acknowledge and thank both ASARCO and Kerr-McGee Corp. for permission to visit their properties and for allowing publication and dissemination of significant exploration data. At this time, when the United States Government is actively suppressing mineral exploration, it is a refreshing contrast to see private companies encourage publication of exploration data and aid in the advancement of applied economic geology.

Enjoy the views of Southeastern Arizona and the Patagonia Mountains as well as the opportunity to see the upper, near-paleo-surface part of porphyry copper alteration systems.

NOTE: The field trip to Red Mountain and the Hardshell Deposit was originally led by James J. Quinlan (Kerr-McGee Corp.), Fleetwood Koutz (ASARCO), and Russell Corn (Consultant) as part of the Arizona Geological Society 1981 Symposium "Relations of Tectonics to Ore Deposits in the Southern Cordillera".

The Hardshell deposit represents exterior silver mineralization related to the Sunnyside porphyry copper alteration center described by Fred Graybeal during the Conference. The Hardshell portion of the field trip will be abbreviated in order to provide time for a trip into the Sunnyside area with a discussion of the geology and alteration - mineralization by Fred Graybeal.

Russ Corn, Dick Ahern, Jim Quinlan, Fred Graybeal

(NOTE: reprinted from 1981 symposium on "Relations of Tectonics to Ore Deposits in the Southern Cordillera", Trip #8)

FIELD TRIP GUIDE

to

RED MOUNTAIN

SANTA CRUZ COUNTY, ARIZONA

Prepared by

James J. Quinlan
Kerr-McGee Corporation

Contents

Page

Illustrations

THIS PAGE

INTENTIONALLY BLANK

ROAD LOG FOR
RED MOUNTAIN PORTION OF
ARIZONA GEOLOGIC SOCIETY FIELD TRIP TO
PATAGONIA-RED MOUNTAIN-HARDSHELL DEPOSITS
MARCH 21, 1981

START

Mile 0.0 — Patagonia, Arizona Post Office at the junction of State Highway No. 82 and county road leading to the San Rafael Valley, Harshaw and Lochiel. Good view of Red Mountain on right.

Mile 1.6 — The Patagonia fault is exposed in outcrop across wash. Fault zone consists of several strands, with consolidated Tertiary gravels on northwest and Meadow Valley Andesite (72.1 ± 3 m.y.) on southeast side of fault zone. Bold outcrops on southeast side of outcrop area are silicified breccias along fault strand in Meadow Valley andesite.

STOP 1

Mile 2.7 — Road cut exposures of Meadow Valley Andesite. These exposures are typical of many Meadow Valley exposures outside of main Red Mountain alteration zone. Would call attention to purple color and propylitic alteration. In core of Red Mountain alteration zone, andesite is typically altered to a black-colored, biotite-magnetite rich rock. Clay and limonite are common along many fractures in the exposures and quartz veinlets and manganese oxides may be seen along some of the fractures.

STOP 2

Mile 4.7 — Locations of Stops 2 through 8 shown on Figure 2. Turn off from San Rafael Valley-Harshaw-Lochiel county road on to road leading to Red Mountain. Will transfer from bus to four-wheel drive vehicles at this point. Outcrops in wash ahead are generally propylitically altered Meadow Valley Andesite. Local bleach zones are mainly controlled by linear structures. Clay, gypsum and limonite are the most common minerals in these zones.

STOP 3

Mile 5.2

View point of southeast side of Red Mountain. Would call attention to route of road leading up mountain, talus covered slopes, land slide blocks and cliffs in upper layered Tuff unit. This upper layered altered Tuff unit is much more resistant to erosion than the underlying andesite and this accounts for the present topographic high at Red Mountain.

STOP 4

Mile 7.1

At outcrop in altered Tuff unit 5,000 feet east of alteration center at Red Mountain (See Figures 2 and 3). Rock is principally clay altered, also note alunite veinlets. Stop is at about outer limit of visible sericite in Red Mountain alteration zone.

STOP 5

Mile 7.5

At collar of Hole No. 158. Road cuts and outcrops of altered Tuff unit ± 2,000 feet closer to Red Mountain alteration center than at Stop 4. Note increase in sericite and pyrite (2 to 2.5 weight %) content over that at Stop 4.

See Map Figures 2 and 3 and Cross Section Figures 4, 6, 10 and 11 illustrating geology, alteration and sulfide changes at and between Stops 5 and 6.

STOP 6

Mile 8.0

Crest of Red Mountain ridge and near collar of Hole No. 151. Road cuts and outcrops of the Tuff unit are inside the area of relative abundant sericite and iron oxides after pyrite. Adjacent drill hole data shows original pyrite content of up to 18 weight percent and an average content of from 10 to 12% (see Figure 6).

STOP 7

Mile 8.8

At collar of Hole No. 148. Road, drill pad cuts and outcrops are in altered Tuff unit, within zone of relatively abundant sericite and iron oxide. Note quartz and alunite veinlets in drill pad cut. Will discuss and point out feature of deposit from view point at this stop. Core specimens illustrating changes in alteration and mineralization with depth will be available at the lunch stop.

STOP 8

Mile 9.0

End of Red Mountain tour-view sight overlooking Hardshell or afternoon tour area.

GEOLOGY AND SILICATE-SULFIDE ALTERATION ZONING AT THE RED MOUNTAIN PORPHYRY COPPER DEPOSIT, SANTA CRUZ COUNTY, ARIZONA

James J. Quinlan

Abstract

This paper is the result of a study of the Red Mountain, Arizona porphyry copper deposit. The bulk of the copper recognized in the deposit lies about 5,000 feet below the summit of the mountain and 3,500 feet below a small, partly dissected, secondary enriched chalcocite blanket.

The copper deposit at Red Mountain occurs within an altered complex of volcanic and intrusive rocks of Cretaceous and early Tertiary age. Silicate alteration, sulfide distribution and assay data have been used to define the deposit and alteration system.

Alteration at Red Mountain is complex. A near classic porphyry-copper silicate-sulfide alteration pattern, including a partially defined copper shell is recognized at depth. This has been superimposed over an earlier potassic alteration assemblage which in turn is a part of a much larger zoned alteration system. Though modified by supergene agents, the early system accounts for much of the alteration recognized at the surface.

The Red Mountain deposit can be divided into three parts: (1) a near surface chalcocite blanket deposit, (2) a deep level bulk sulfide deposit and (3) a copper-molybdenum breccia pipe within the core area of the deep porphyry copper system.

The most obvious clue to the deep orebody at Red Mountain is the shallow chalcocite blanket. This apparently has formed from a low grade copper halo or plume which extends upward to the present surface or at least 5,000 feet above the deep orebody.

Introduction

The Red Mountain copper deposit is at the northern end of the Patagonia Mountains, 50 miles southeast of Tucson, Arizona (Fig. 1). The deposit was discovered and is controlled by the Kerr-McGee Corporation of Oklahoma City, Oklahoma.

The bulk of the copper recognized in the deposit lies about 5,000 feet below the summit of the mountain and 3,500 feet below a partly dissected enriched chalcocite blanket.

The geology of the Red Mountain deposit and surrounding area has been described by a number of authors. The most pertinent publications are: Schrader (1915), Drewes (1971 A & B and 1972 A & B), Simons (1971 and 1974), Corn (1975) and Bodnar and Beane (1980).

Geology

Geologic Setting

Red Mountain is underlain by an altered complex of volcanic and intrusive rocks of Cretaceous and early Tertiary age. Figures 2 and 3 are generalized maps illustrating surface geology and alteration features. Figures 4 and 6 are diagrammatic cross sections showing geologic and alteration features.

Three layered volcanic units are recognized at Red Mountain. The upper or Tuff unit, consists mainly of tuffs, flows and breccias of rhyolitic and dacitic composition. It crops out over much of the mountain and is up to 2,400 feet thick (Fig. 2 and 4). It is essentially the same as the "Volcanics of Red Mountain" described by Drewes (1971 A) and which he correlates with the Gringo Gulch volcanics of Paleocene (?) age.

Underlying the Tuff unit are approximately 3,000 feet of andesite and trachyandesite flows, breccias, sills and dikes locally referred to as the Andesite unit. Hornfels bands occur near the base of the unit. The Andesite unit crops out on the flanks of Red Mountain and is cut in drill holes (Fig. 2 and 4). It is a part of the upper Cretaceous Trachyandesite or Doreite (Ka) unit, mapped and described by Simons (1974). Simons reports a potassium argon date of 72.1± three million years for a sample from the unit.

The lowest layered rock unit is the Felsite-Latite unit. It underlies the Andesite unit and includes interlayered andesites near the top. It consists mainly of volcanic conglomerates and breccias, silicified tuffs, flows(?), interlayered and cut by latite sills and dikes. The unit crops out in Alum Gulch on the south side of Red Mountain and is recognized in deep drill holes on the south and west flanks of the mountain (Fig. 2 and 4). It correlates with the upper Cretaceous Silicic Volcanics (Kv and Kla units) mapped by F. S. Simons (1974).

The layered rocks at Red Mountain are cut by several textural varieties of porphyritic rocks which range in composition from granodiorite to quartz monzonite. The porphyries are recognized as dikes and irregular bodies in outcrop and drill holes (Fig. 2 and 4).

The layered rocks generally strike north and dip 15° E. The dominant trend of local shears and fractures is N 20° E with steep dips toward the northwest and southeast. Less numerous are shears and fractures which strike N 70° E and dip steeply northwest or southeast. No large faults are recognized on the mountain but several occur on its flanks (Fig. 2).

Silicate Alteration

Silicate alteration at Red Mountain is easy to recognize but difficult to interpret. Near the center of the deposit, changes in the alteration assemblage with depth are most obvious (Fig. 6). Lateral zoning at depth, which is a critical guide to ore, is much more subtle and to date has been best quantified by thin section studies (Fig. 5).

The strong vertical alteration zoning recognized at Red Mountain is partly controlled by differences in rock types with depth. Near the center of the system, the Tuff unit is intensely altered to an assemblage of quartz-sericite-pyrite-kaolinite-alunite. The sericite content increases with depth while the content of kaolinite and alunite decreases. At the Tuff-Andesite contact, the assemblage abruptly changes to quartz-sericite-chlorite-pyrite with minor hematite and kaolinite. With the exception of outlying Hole 158, the pyrite content rapidly decreases in depth through the upper Andesite interval (Fig. 10). The alteration assemblage further changes with depth within the andesite through a biotite-magnetite-pyrite assemblage to a biotite-orthoclase-anhydrite-magnetite-chalcopyrite assemblage. Within the Felsite-Latite unit, the assemblage is orthoclase-quartz-anhydrite-chalcopyrite-biotite. The alteration within the porphyritic rocks is generally reflective of the adjacent intruded rock and depth. It is expressed by a quartz-sericite-pyrite-kaolinite assemblage at shallow depths and an orthoclase-anhydrite-biotite-chalcopyrite assemblage at greater depth.

Lateral changes in alteration are much more subtle. At the surface hypogene alteration is strongly masked by supergene effects but is discernible. Within the Tuff unit, the lateral zoning is expressed as a central core area of more abundant sericite, quartz veining and limonitic stain (Fig. 3). Outward from the core area, a more argillic zone is characterized by abundant clays and alunite with less sericite and silica. The transition from sericitic-argillic alteration within the Tuff unit to propylitic alteration in the surrounding andesite to the northeast, east, south and southwest appears to be partly due to change in rock type. The suggestion is that the alteration mushroomed or extended farther laterally from a mineralization center in the Tuff unit than in the underlying andesite. Within the andesite on the west and northwest flanks of the mountain an intense supergene argillic alteration is superimposed directly upon hypogene biotite-magnetite alteration. Within this area of relatively low original pyrite, chalk turquoise has formed as the more common supergene copper mineral within the argillized andesite.

At depth, the central core area is marked by an orthoclase-quartz-biotite-anhydrite alteration mineral assemblage. There is a general decrease in the amount of these minerals outward from the core area with increasing amounts of sericite and chlorite. This is illustrated on Figure 5 which was developed from a study of thin sections obtained from selected holes between elevations of 2,000 and 2,500 feet.

Farther out, as seen in Holes 157 and 161, a biotite-magnetite assemblage is recognized in the andesite. In Hole 157, this assemblage changes to biotite-orthoclase in the Felsite-Latite unit. Though the assemblage is potassic, the intensity of the potassic alteration appears much less than that recognized in the core area of the deposit. Locally, late quartz-pyrite veinlets enclosed in sericitic envelopes cut the previously described alteration features.

Figure 6 illustrates in cross section the writer's concept of the major silicate alteration features at Red Mountain. That is, a large early zoned alteration system which accounts for most of the alteration recognized at the surface. The primary porphyry copper deposit lies in the potassic zone of this large early system. The alteration associated with the primary deposit has been superimposed on the early alteration system and zoning is similar to that described by J. D. Lowell and J. M. Guilbert (1970) and A. W. Rose (1970). It is suspected that the two silicate alteration systems are closely related in origin and time with the porphyry copper phase representing a late event in the development of the complex Red Mountain hydrothermal system. The sulfide distribution data also clearly points to two distinct alteration phases as does the fluid inclusion data of Bodnar and Beane (1980).

Sulfide Distribution

The principal sulfide minerals at Red Mountain are pyrite and chalcopyrite. Secondary chalcocite is present, particularly in the blanket deposit. Small amounts of molybdenite are present and bornite, enargite, tennantite, galena and sphalerite have been identified locally.

The sulfide content of the rocks at Red Mountain has been estimated during core logging and in the deep holes has been determined on the basis of sulfur and sulfide sulfur assays.

For the purposes of the sulfide distribution studies, it has been assumed that pyrite and chalcopyrite are the only significant primary sulfide minerals in the Red Mountain system. The amounts of each below the zone of secondary enrichment are calculated from copper and sulfide sulfur data by assigning the amount of sulfide sulfur needed to convert the amount of copper present in an interval to chalcopyrite and assigning the remaining sulfide sulfur to pyrite. Sulfate data has been converted to anhydrite equivalent where anhydrite is recognized in the deep drill holes.

The sulfide data has been assembled and posted in several different manners on plans and cross sections, i.e., by rock type and at various elevation intervals. Most revealing is the bulk data when assembled and posted at elevation intervals of 500 feet or more. In general, plans and sections have been prepared showing pyrite, chalcopyrite, and total sulfide (combined pyrite and chalcopyrite) distribution and pyrite to chalcopyrite ratios. The pyrite and total sulfide maps and sections are so reflective of each other that maps and sections showing pyrite distribution have not been included with this report.

Plan illustrations accompanying the report show relative bulk chalcopyrite (Fig. 7) and total sulfide distribution (Fig. 8) and relative pyrite to chalcopyrite ratios (Fig. 9) between elevations of 500 and 1,500 feet. All three maps show the same basic pattern and closely match the silicate alteration pattern shown in Figure 5. Though drilling has yet to outline the entire system, available data indicates an elongate but nearly classic sulfide copper shell. Thus all three plans, and in particular the ratio map (Fig. 9), are useful in indicating where a drill hole lies within the system.

Cross sections prepared from the sulfide data, i.e., data assembled at 500-foot elevation intervals, not only confirm the picture developed in plan but add to it. Total sulfide and chalcopyrite data have been assembled on Section A-A' which passes through the core area of the lower sulfide system as well as outlying Holes 157 and 158 (Fig. 10 and 11). The section showing total sulfide distribution (Fig. 10) clearly demonstrates a two-part system. A large primary sulfide high, mostly pyrite, is recognized near the surface in the upper parts of the central drill area and in Hole 158. This pyrite is within and generally an integral part of the intense quartz-sericite alteration assemblage. The section also suggests that Hole 157 lies in the core area of the large primary sulfide system and would account for the potassic alteration recognized in the hole. It is also apparent that the strong iron oxides recognized on the upper western slope of Red Mountain (Fig. 3) are related to the upper sulfide system.

The copper system recognized at depth in the central drill area and shown on the sulfide distribution and ratio maps (Fig. 7-9) is also apparent in the cross sections showing the total sulfide and chalcopyrite distribution (Fig. 10 and 11). Although the amount of total sulfides in the lower system (Fig. 10) is less than that in the upper system, it is clear from Figure 11 that the copper is associated with the lower system. Further it is apparent in section that the lower sulfide system closely follows the central area silicate system and like the silicate system is superimposed on the earlier and larger system.

The Ore Deposit

For discussion purposes, the Red Mountain deposit is divided into three separate and distinct parts: (1) an upper level chalcocite blanket deposit, (2) a deep level bulk sulfide deposit and (3) a breccia pipe deposit within the core area of the deep porphyry copper system.

Chalcocite Blanket

Chalcocite is recognized along fractures and as coatings on pyrite grains from the surface to a depth of 2,500 feet or more. Much of the chalcocite appears to be concentrated in a flat blanket-like deposit near an elevation of 5,000 feet (Fig. 11). As currently defined, the blanket ranges in thickness from 15 to 150 feet. It appears to be in the process of being destroyed by weathering and erosion and the deeper scattered chalcocite showings which are usually controlled by fissures or shears probably represents recent copper migration.

The chalcocite blanket almost directly overlies the deep porphyry copper orebody (Fig. 3 and 11). The distribution of copper above the deep porphyry copper system as reflected by the relative copper or chalcopyrite values shown in Figure 11, suggests the blanket was formed by enrichment of a protore halo or plume extending at least to the present surface or 5,000 feet above the main ore system. Bodnar and Beane's (1980) description of the late stage of mineralization in a quartz-pyrite veinlet containing minor chalcopyrite and galena in a surface sample, RM 11, also is evidence that the ore stage primary mineralization extends far above the main deposit.

The zone of deep level porphyry copper mineralization at Red Mountain is an integral part of the copper shell as recognized in the alteration and sulfide study. Holes 146, 165 and the deeper parts of Hole 144 describe the low-sulfide, low-copper core of the system. A low-sulfide, low-copper tail extends from the core and is recognized in seven holes, 133, 135, 154, 162, 147, 143 and 152. A breccia pipe is defined in Holes 148, 148B, 148C and 155 and lies within the elongated tail area.

Nine drill holes are immediately peripheral to the core area and the elongated tail and it is in the area of these nine holes that most of the deep level copper outside the breccia pipe occurs. Seven of the nine holes contain thick and/or higher grade ore intervals. Ore is recognized on both the west and east limbs of the copper shell (Fig. 4).

Much, if not most, of the deep level copper occurs as chalcopyrite along veinlets and fractures and only a small amount occurs as disseminated grains. From work to date, it is obvious that the area of the copper shell is not uniform in grade and everywhere of interest. Local controls and structure apparently played an important part in copper mineralization within the shell area. For example, chalcopyrite enrichment is noted along both sides of andesite-porphyry contacts in several holes.

148-155 Breccia Pipe

The 148-155 breccia pipe recognized at Red Mountain has many features common to mineralized breccia pipes at other porphyry copper deposits. It is perhaps the deepest copper-molybdenum breccia pipe presently known anywhere in the world. Not only is it of potential economic interest because of the higher grade ore associated with it, but it is also of considerable scientific interest because of its depth, position within the system, and the mineralization and alteration associated with it.

The Dyna-drill has been used to control the direction of drill holes for a better evaluation of the pipe. In all, four holes have intersected the pipe, Holes 148, 148B, 148C and 155 (Fig. 12).

The 148-155 breccia pipe, as envisioned from drill hole data, is shown in plan and diagrammatic section in Figure 12. Though in part diagrammatic, the plan and section represent a reasonable interpretation based on drill hole intercepts within the pipe and the confining restrictions of adjacent holes. In plan the intercepts in Holes 148 and 155 are about 800 feet apart and define the minimum dimension of the long axis of the pipe. The pipe has been assigned a long axis of 1,100 feet. The section better illustrates the information available. As shown, the top of the pipe is at an elevation of 1,750 feet or approximately 4,000 feet below the surface and ore has been exposed over a vertical range of 1,300 feet. Hole 148 bottoms in ore within the pipe near sea level elevation.

As mentioned before, the 148-155 pipe lies within the high-potassic, low-sulfide and low-copper tail extending southward from the core of the deep porphyry copper system (Fig. 9). The alteration within the pipe is separate and generally distinct from that of the surrounding rock. This is well exemplified in Holes 148B, 148C and 155. These holes enter the pipe near its top from an area of low-sulfide, low-copper and strong potassic alteration. At or within a few feet of the pipe contact, alteration abruptly changes to phyllic with abundant sericite and up to 30 percent by weight of pyrite. Strong phyllic alteration persists near the top of the pipe but gives way to potassic alteration with depth. Only in hole 155 is a significant amount of possible mineralization leakage recognized above the pipe. Though the pipe contact in this hole is sharp and distinct, bands of pipe-type mineralization are evident for 40 feet above the pipe. Shears with chlorite, sericite and quartz-sulfide veinlets similar to pipe mineralization are recognized up to 775 feet above the pipe.

Unlike many breccia pipes described in the literature, the mixing and movement of fragments great distances up or down the pipe has not been recognized in the 148-155 breccia pipe. Though fragments are broken and rotated, the composition of fragments, with but a few exceptions, appear to be similar to those in the immediate wall of the pipe. More detail is needed to substantiate this observation.

The ore breccia generally consists of angular fragments of felsite and andesite in a matrix of orthoclase, quartz, anhydrite, chalcopyrite and pyrite. Sericite is abundant near the top and also is recognized close to the sides of the pipe in deeper intercepts. Calcite, molybdenite and a dark gray sulfosalt, tenatively identified as tennantite, are accessory minerals. Breccia fragments are commonly an inch or less in diameter. The largest fragment recognized was 18 inches in diameter. Open vugs are common.

A definite enrichment of copper, molybdenum and silver is recognized at the pipe margin, particularly in the deeper intercepts. The enrichment is related to the concentration of chalcopyrite and molybdenite rich sulfide lenses at the margins. The grade of copper at the margins of the pipe is from 1.8 to 4.8 times that in the core area of the pipe. Molybdenum enrichment at the margins is ten times and that of silver from two to four times that of the pipe core.

The silicate alteration and sulfide distribution pattern recognized in the pipe, though different in scale, is much the same as that recognized in many large porphyry copper systems, that is, a core area of strong potassic alteration with lower sulfide content. This is followed upward and to a lesser extent outward towards the pipe margins by a phyllic zone with increased sulfides. The suggestion is that the pipe itself may represent a more intense but miniature zoned porphyry copper system superimposed over the main or bulk phase of porphyry copper alteration and mineralization.

Discussion

Most of the alteration recognized at the surface of Red Mountain results from the supergene modification of a large zoned hypogene alteration system formed prior to the emplacement of the deep porphyry copper deposit.

The deep level porphyry copper is related to a more intense, less extensive event in the evolution of the complex hydrothermal system. The superposition of the breccia pipe alteration and mineralization over the main phase porphyry copper alteration and mineralization indicates an even more confining, more intense alteration, mineralization pulse late in the evolution of the system.

Though the three hydrothermal events appear separate and distinct, all three are undoubtedly closely related in time and origin to each other and to the emplacement of porphyry intrusives at Red Mountain. The indicated sequence of formation appears to start with the development of the large, barren, zoned system, with succeeding but more restrictive and intense pulses of ore mineralization within the confines of the large barren system.

The zoned nature of alteration and mineralization within the breccia pipe indicates the pipe itself may represent a miniature zoned porphyry copper system. Whereas the pipe contains open vugs, most evidence indicates that it must have formed many thousands of feet below the surface.

The most obvious clue to the deep orebody at Red Mountain is the shallow chalcocite blanket. This appears to have formed from a low-grade copper halo or plume which extends upward to the present surface or at least 5,000 feet above the deep orebody. Undoubtedly, pyrite from the early alteration system played an important part in the generation of acid for leaching of the plume mineralization.

References

Bodnar, R.J., and Beane, R.E., Temporal and spatial variations in hydrothermal fluid characteristics during vein filling in preore cover overlying deeply buried porphyry copper-type mineralization at Red Mountain, Arizona: Econ. Geol., v. 75, pp. 876-893.

Corn, R.M., 1975, Alteration-mineral zoning, Red Mountain, Arizona: Econ. Geol., v. 70, pp. 1437-1447.

Drewes, Harold, 1971 A, Geologic map of the Mount Wrightson Quadrangle, southeast of Tucson, Santa Cruz and Pima Counties, Arizona: U.S. Geol. Survey Misc. Geol. Inv. Map I-614.

__________, 1971 B, Mesozoic stratigraphy of the Santa Rita Mountains, southeast of Tucson, Arizona: U.S. Geol. Survey Prof. Paper 658-C.

__________,1972 A, Cenozoic rocks of the Santa Rita Mountains, southeast of Tucson, Arizona: U.S. Geol. Survey Prof. Paper 746.

__________, 1972 B, Structural geology of the Santa Rita Mountains, southeast of Tucson, Arizona: U.S. Geol. Survey Prof. Paper 748.

Lowell, J.D., and Guilbert, J.M., 1970, Lateral and vertical alteration-mineralization zoning in porphyry ore deposits: Econ. Geol., v. 65, pp. 373-408.

Rose, A.W., 1970, Zonal relations of wallrock alteration and sulfide distribution of porphyry copper deposits: Econ. Geol., v. 65, pp. 920-936.

Schrader, F.C., 1915, Mineral deposits of the Santa Rita and Patagonia Mountains, Arizona, with contributions by J.M. Hill: U.S. Geol. Survey Bull. 582.

Simons, F.S., 1971, Mesozoic stratigraphy of the Patagonia Mountains and adjoining areas, Santa Cruz County, Arizona: U.S. Geol. Survey Prof. Paper 658-E.

__________, 1974, Geologic map and sections of the Nogales and Lochiel Quadrangle, Santa Cruz County, Arizona: U.S. Geol. Survey Misc. Inv. Series I-762.

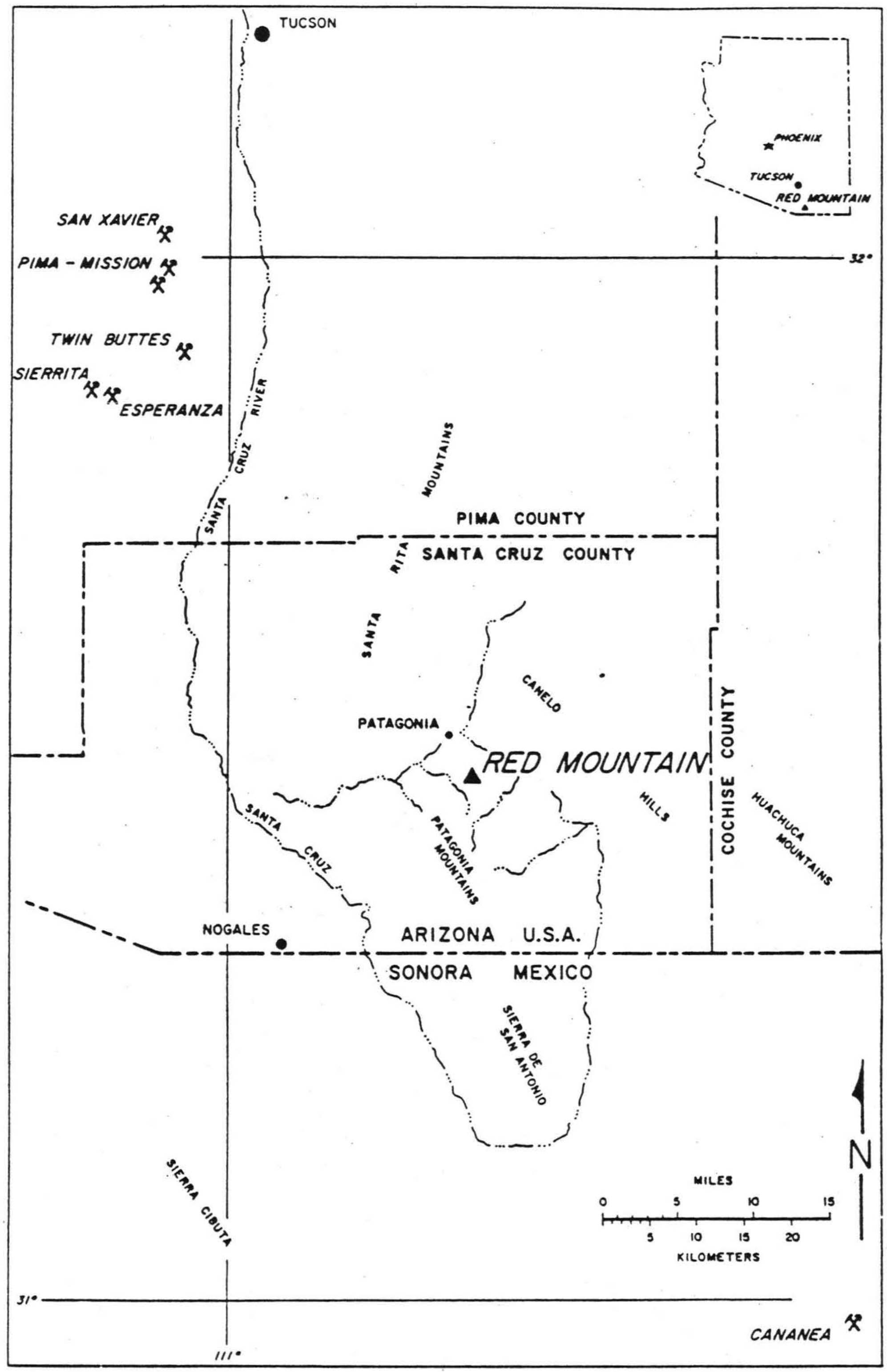

Fig. 1. Index map showing the location of the Red Mountain porphyry copper deposit. After R.M. Corn, Economic Geology, Vol. 70, No. 8, Dec. 75

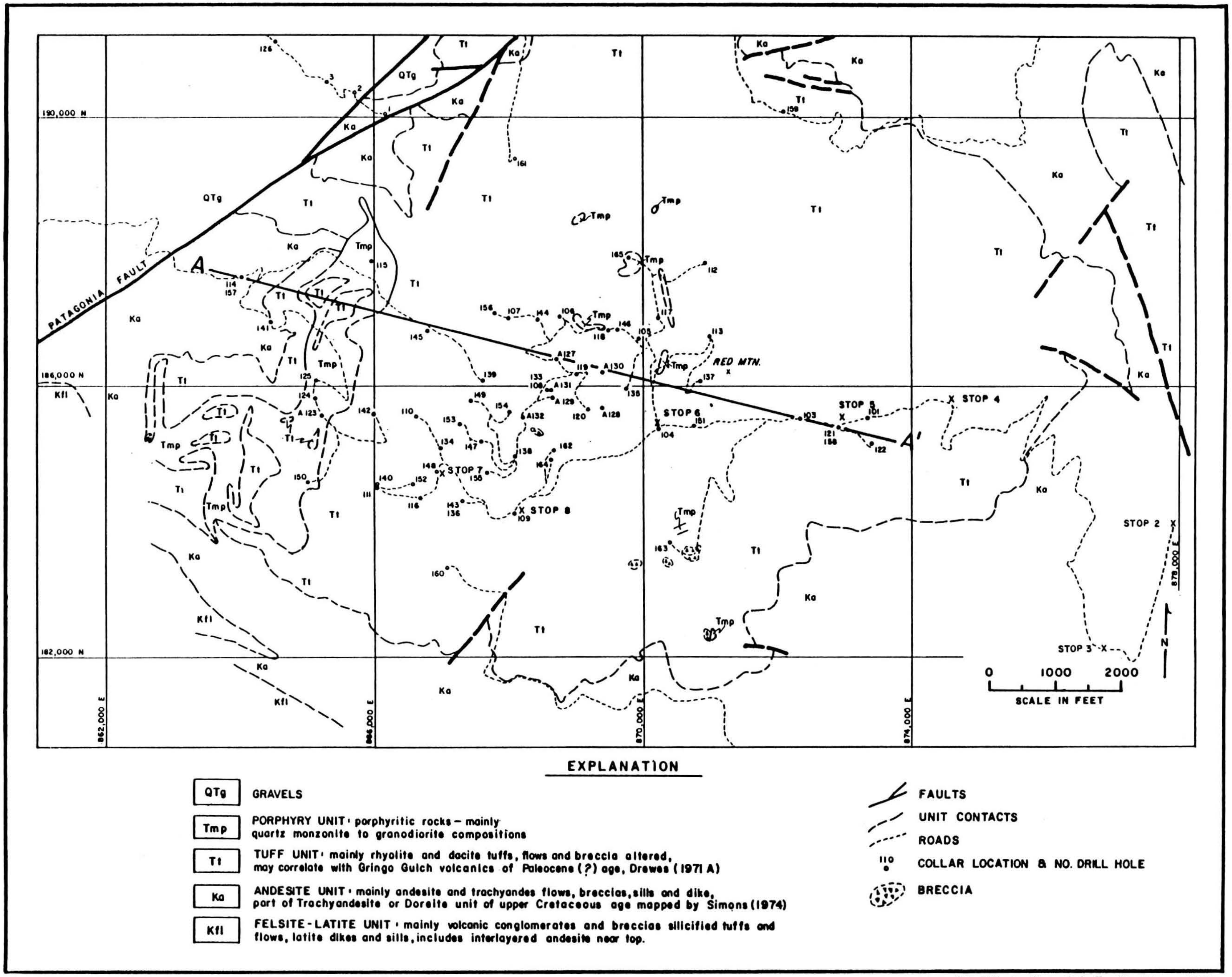

Fig. 2. Generalized surface geologic map of Red Mountain, Arizona. Modified after D.L.E. Huckins, 1975.

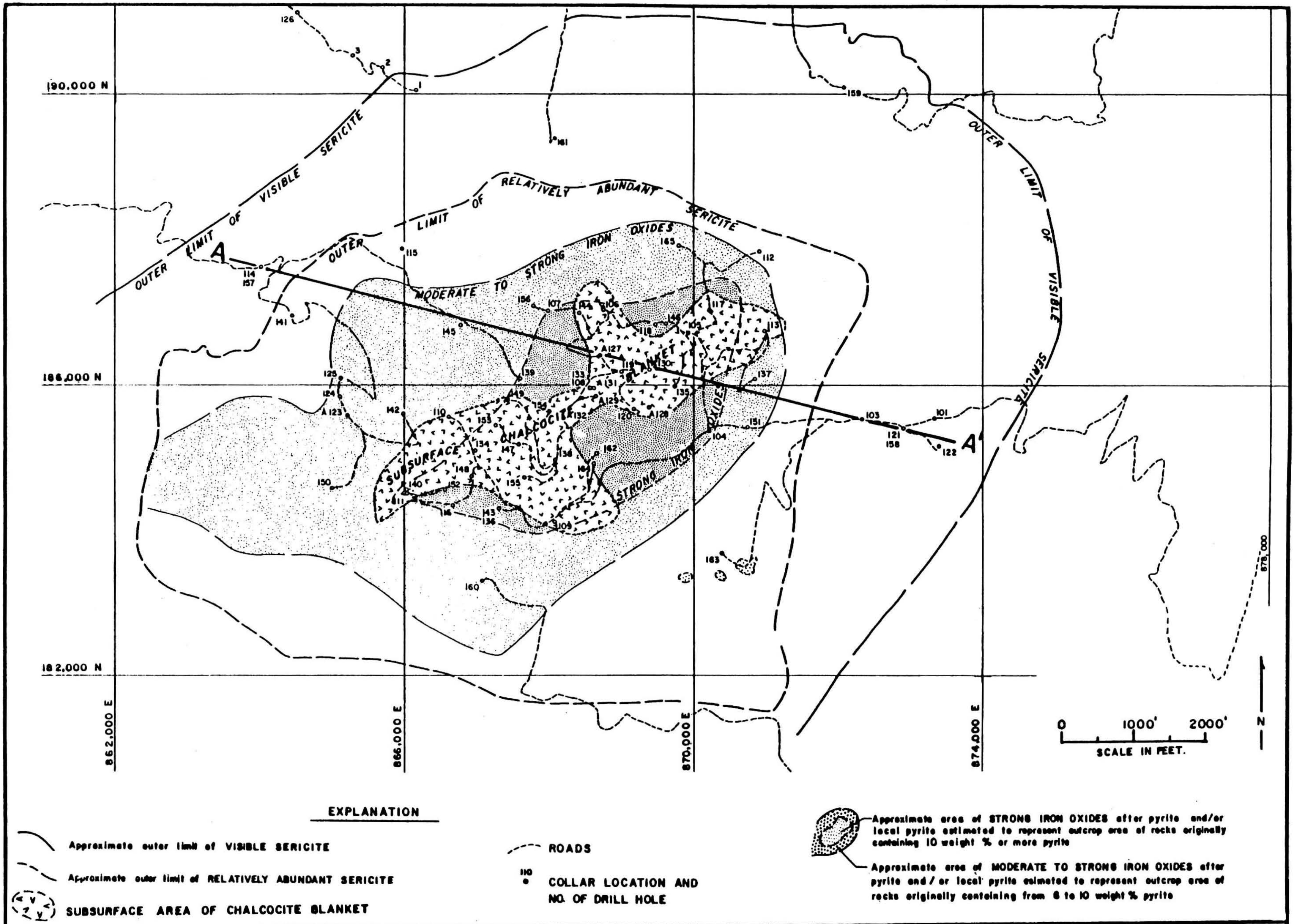

Fig. 3. Generalized surface alteration map of Red Mountain, Arizona.

Modified after D.L.E. Huckins, 1975.

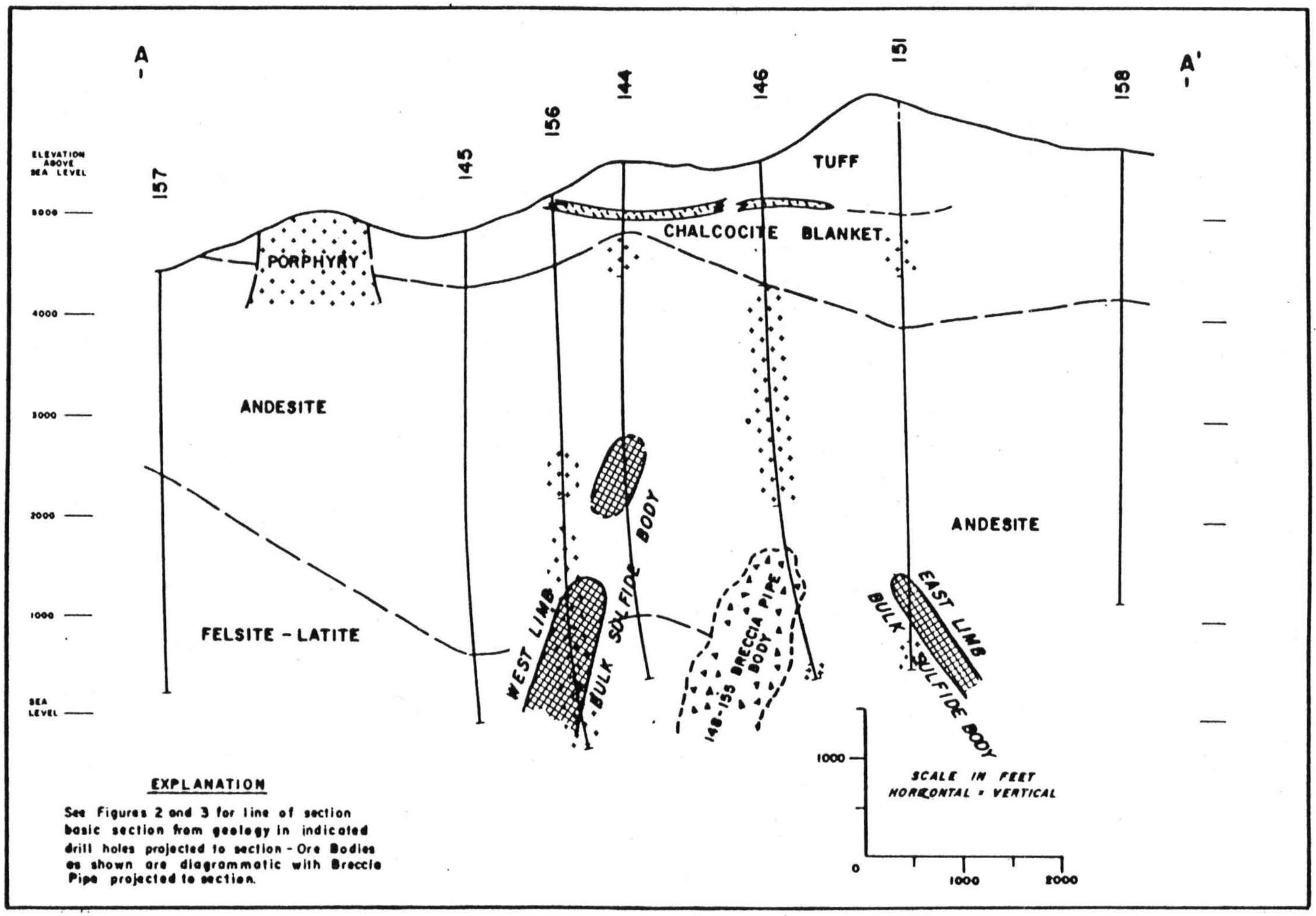

Fig. 4. cross—section A—A'. looking northeasterly, diagrammatically showing geology at Red Mountain, Arizona .

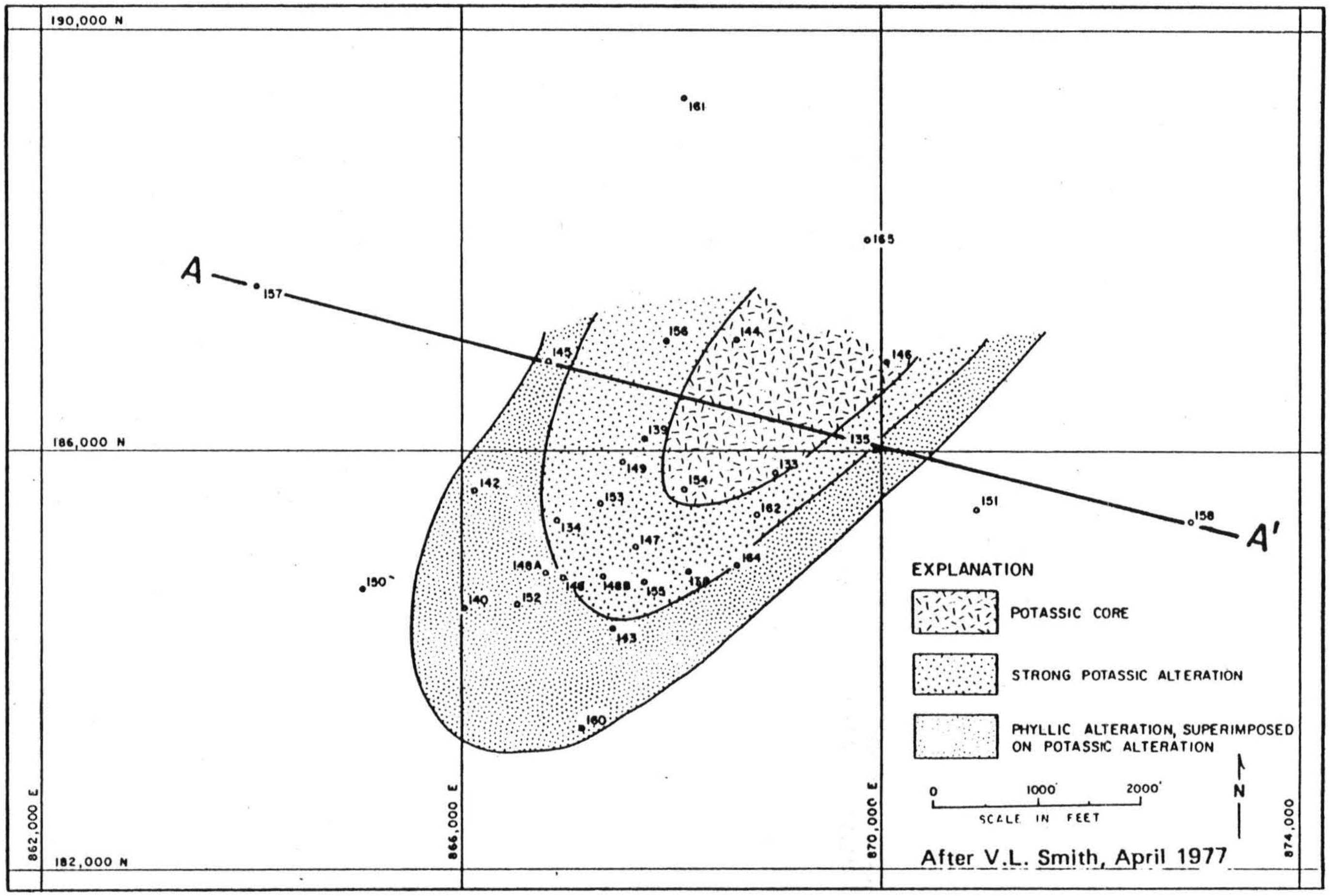

Fig. 5. Map showing silicate alteration between elevations 2,000' and 2,500' at Red Mountain, Arizona. Developed from petrographic study of thin sections from selected holes.

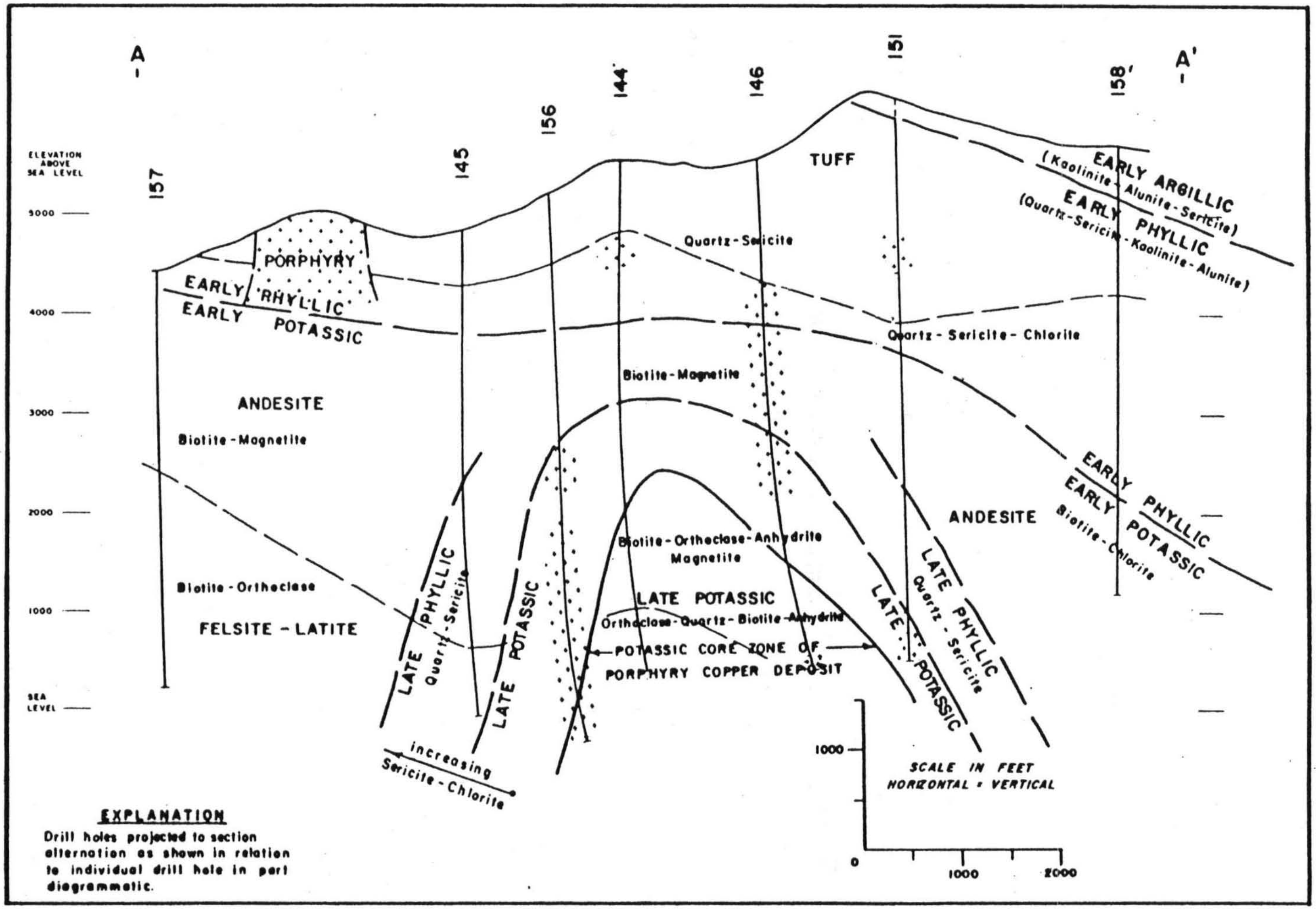

Fig. 6. Cross section A–A', looking northeasterly, diagrammatically showing silicate alteration at Red Mountain, Arizona.

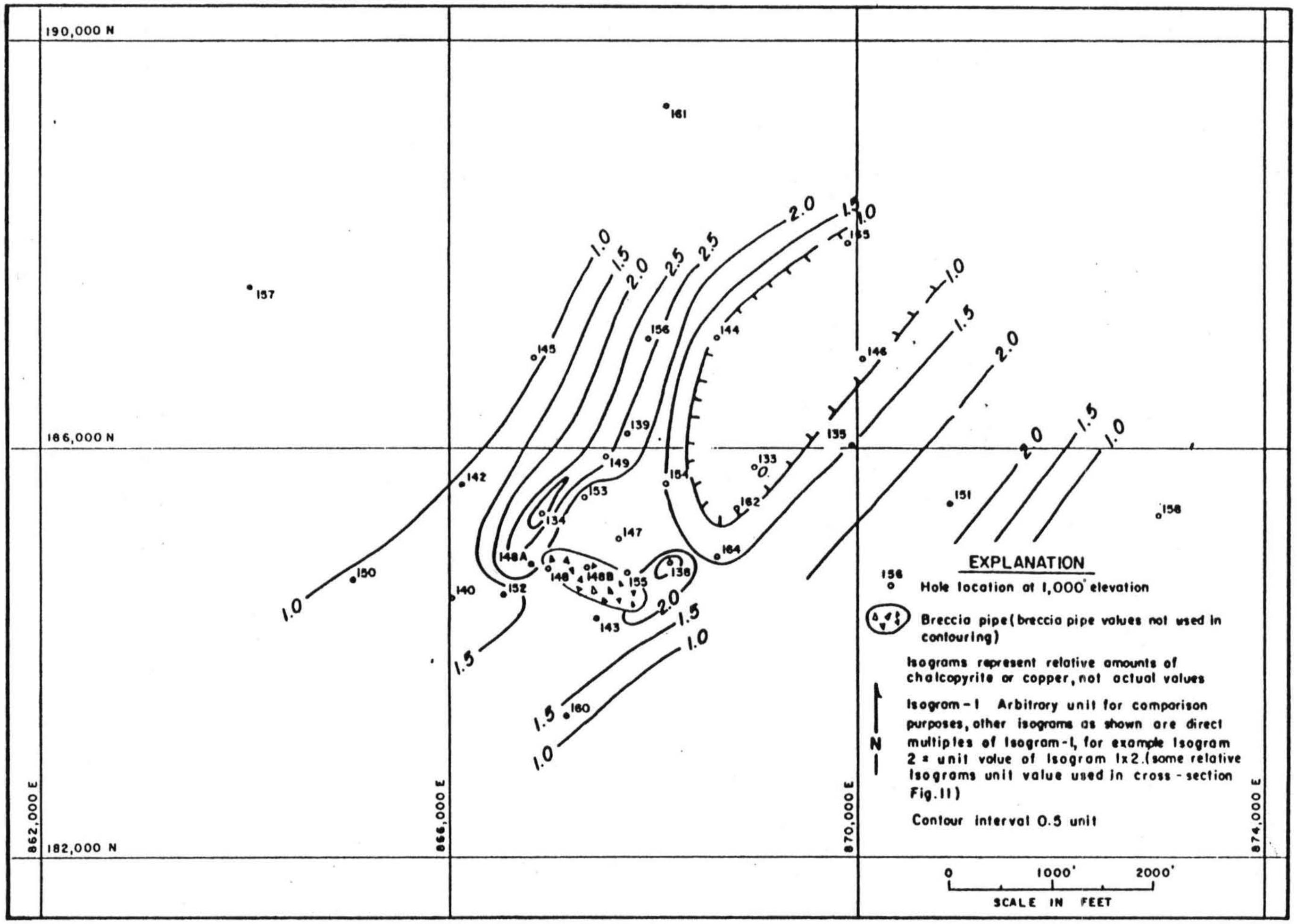

Fig. 7. Map showing relative chalcopyrite distribution between elevations 500' and 1,500' at Red Mountain, Arizona.

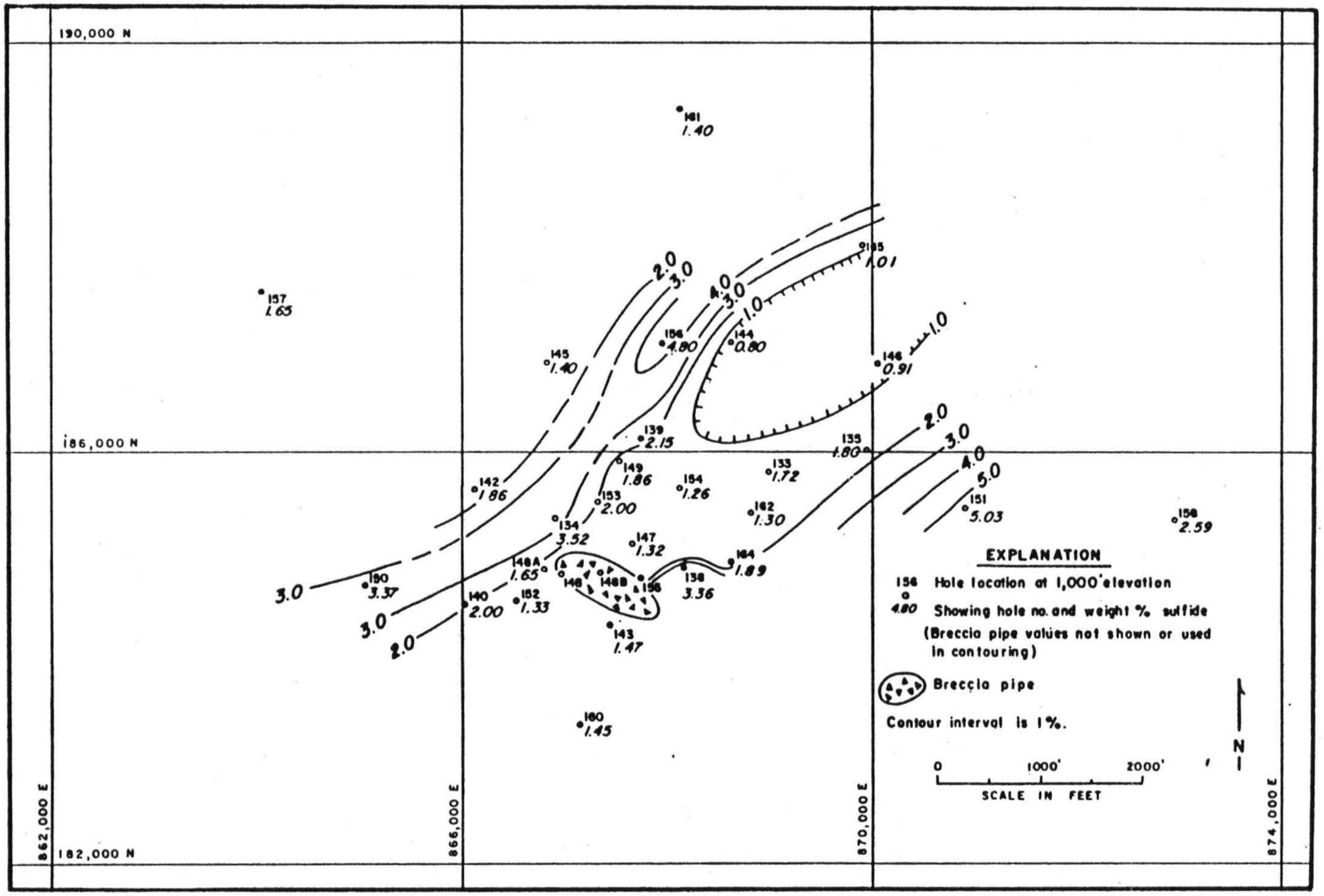

Fig. 8. Map showing total sulfide distribution between elevations 500' and 1,500' at Red Mountain, Arizona.

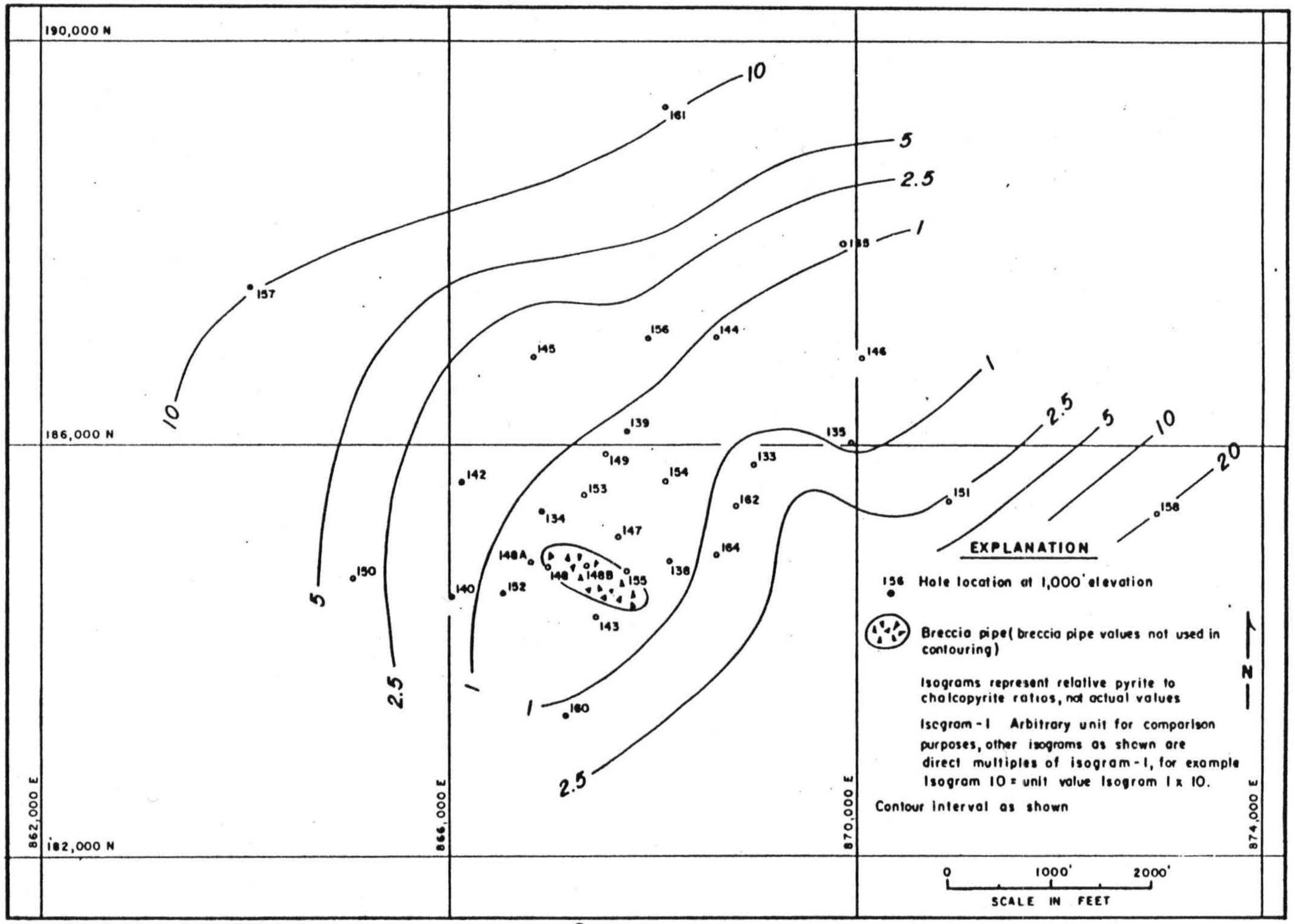

Fig. 9. Map showing relative pyrite / chalcopyrite ratios between elevations 500' and 1,500' at Red Mountain, Arizona.

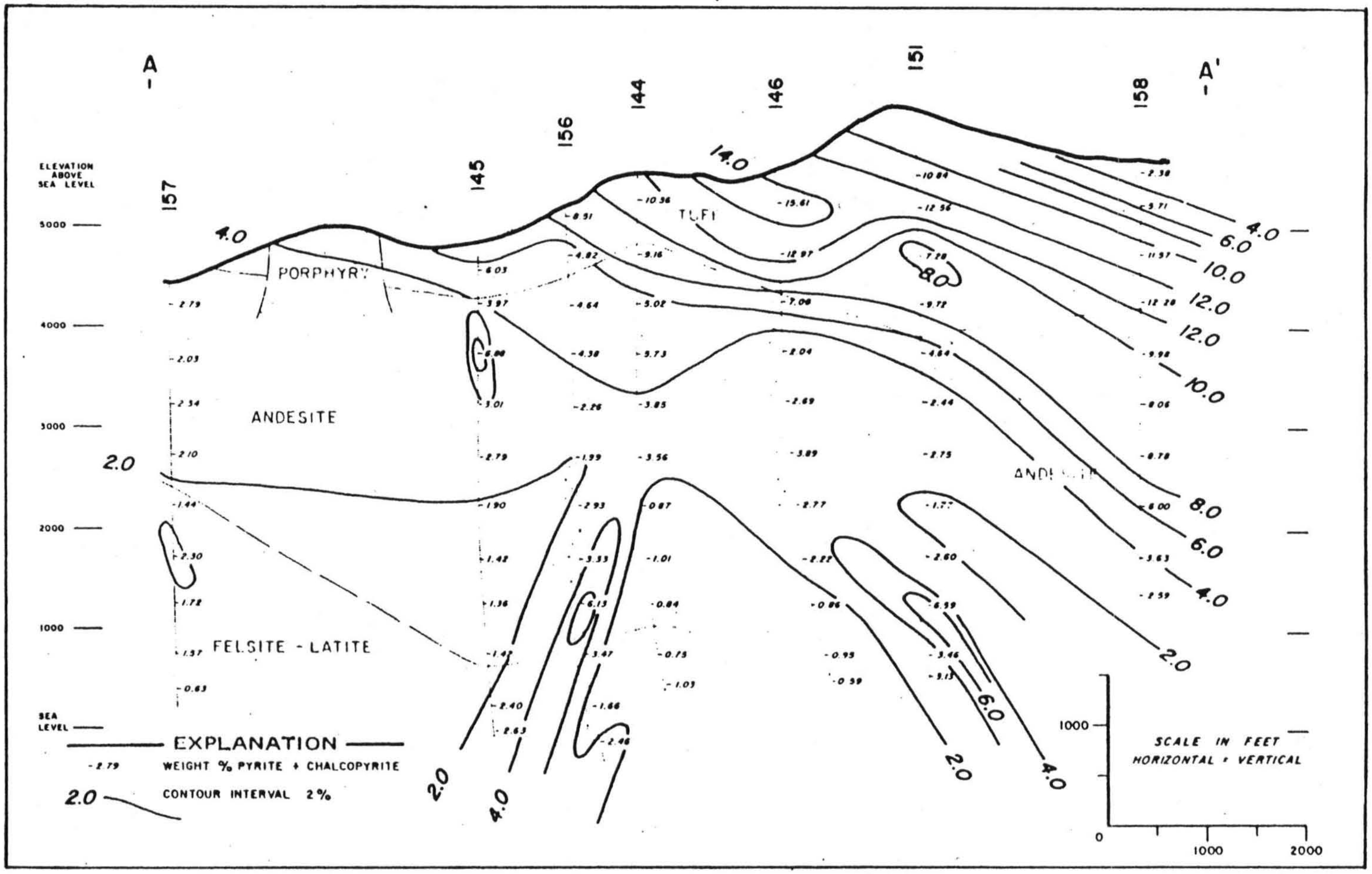

Fig. 10. Cross section A—A', looking northeasterly, showing total sulfide distribution at Red Mountain, Arizona.

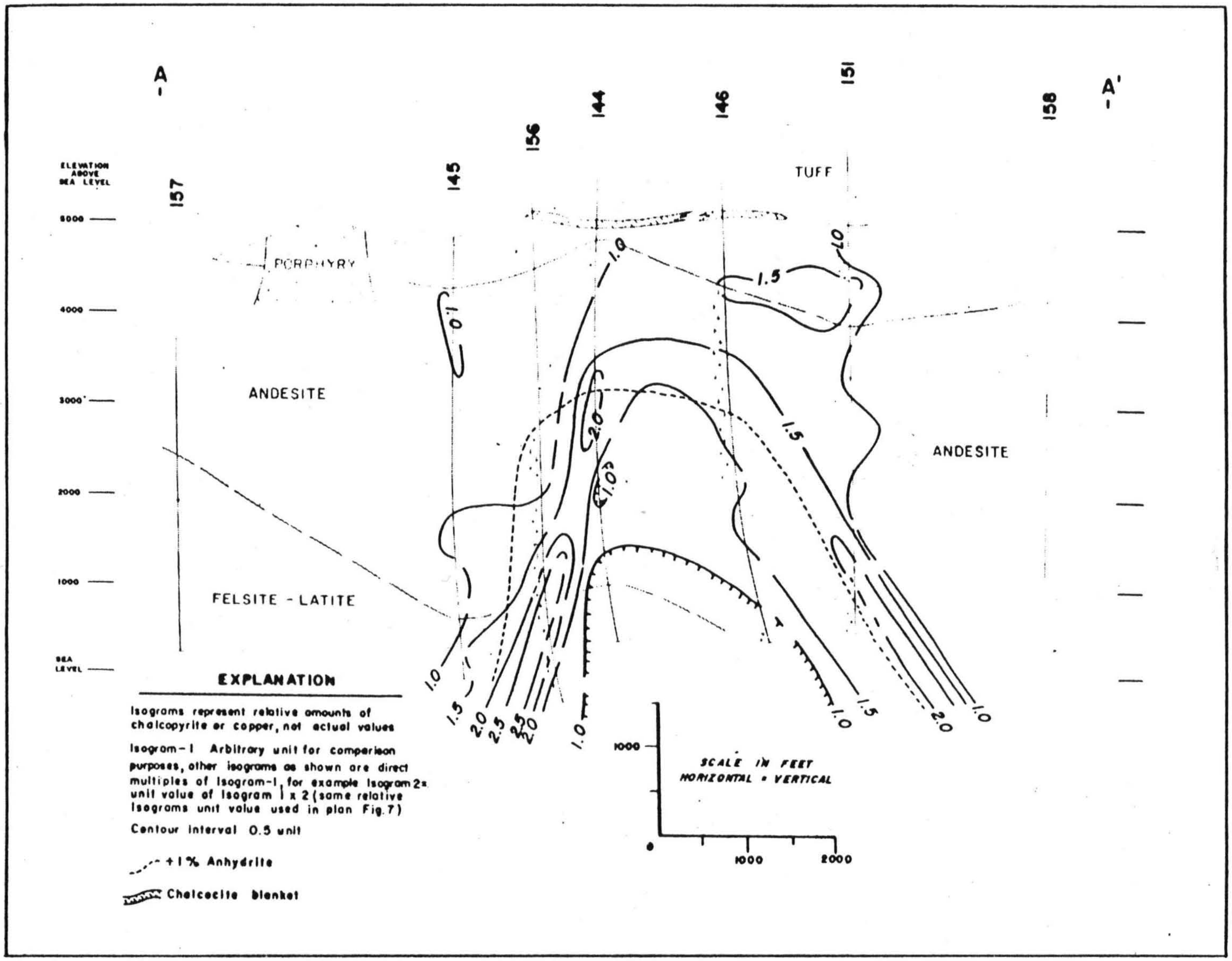

Fig. 11. Cross section A–A', looking northeasterly, showing relative chalcopyrite and anhydrite distribution at Red Mountain, Arizona.

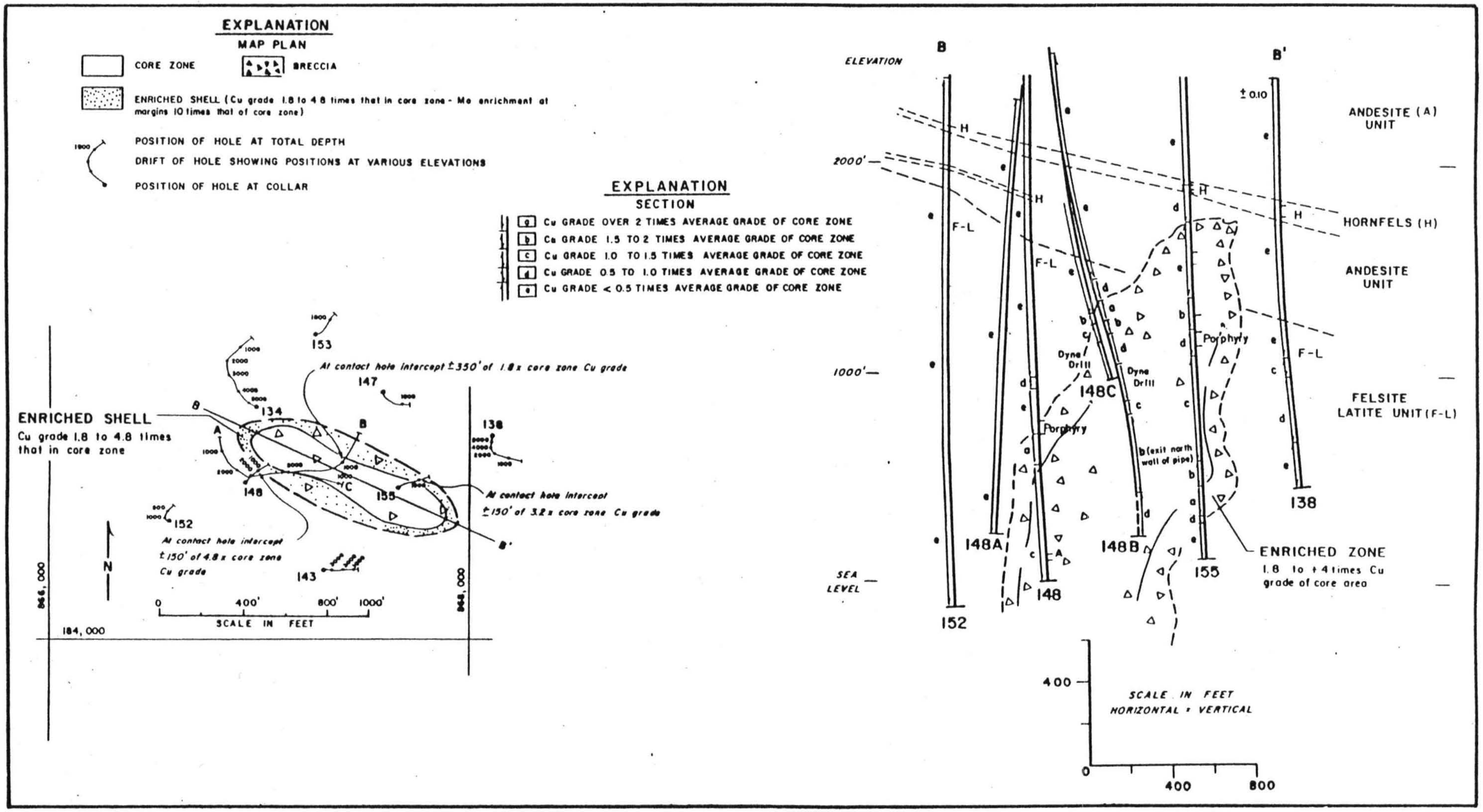

Fig. 12. Plan map and diagramatic cross section, looking northeasterly 148–155 breccia pipe at Red Mountain, Arizona.

THIS PAGE

INTENTIONALLY BLANK

THE HARDSHELL SILVER, BASE-METAL, MANGANESE OXIDE DEPOSIT PATAGONIA MOUNTAINS, SANTA CRUZ COUNTY, ARIZONA: a Field Trip Guide

CONTENTS

(NOTE: The following paper is reprinted from Arizona Geological Society Digest Volume 15, 1984, p. 199 -217.)

THIS PAGE

INTENTIONALLY BLANK

The Hardshell Silver, Base-metal, Manganese Oxide Deposit, Patagonia Mountains, Santa Cruz County, Arizona: a Field Trip Guide

Fleetwood R. Koutz
Southwestern Exploration Division
ASARCO Incorporated
P. O. Box 5747
Tucson, AZ 85703

ABSTRACT

This field trip guide describes the altered and mineralized volcanic host rocks marginal to and above one of the larger silver deposits in the United States. The Hardshell deposit formed as the result of oxidation of a manganese-rich sulfide deposit which had previously replaced permeable Cretaceous ash-flow volcanics and Paleozoic sediments. Both high-angle structure and stratigraphy played a significant role in localizing mineralization but mineralization as a whole is part of a zoned system in the Northern Patagonia Mountains.

INTRODUCTION

This field trip guide was originally prepared for the afternoon portion of Arizona Geological Society Field Trip 8, held on March 21, 1981 as part of the Symposium: "Relationships of Tectonics to Ore Deposits in the Southern Cordillera" held in Tucson on March 19-20, 1981 (AGS Digest XIV). Because of the limited distribution of the field trip guide and lack of space for all of those who had wished to go on the trip the original field trip guide is reproduced here with only minor modifications.

This field trip examines the Hardshell deposit, a large, low-grade silver, base-metal manganese oxide occurrence on the margins of a zoned, base and precious metal district in the Northern Patagonia Mountains (Figs. 1 & 2).

The history of mining in the district, the discovery of the Hardshell orebody, and regional stratigraphy were discussed at the lunch stop (A). Portions of the volcanic stratigraphy, controlling structure, and the mineralized and altered section in Hardshell Canyon can be examined by walking essentially down-section to the outcrop of the upper fringes of the main orebody (stops B - G). A drive to Hardshell Ridge, several hundred feet above Hardshell Canyon, examined the altered and mineralized volcanics (stop H) overlying the crest of the main orebody (Figs. 3, 4, 5).

SUMMARY

Exploration at Hardshell by Asarco has outlined in excess of 6 x 10^6 tons of near-surface mineralization containing about 5 oz. Ag/T, less than 0.01 oz. Au/T, several percent total Pb and Zn, and about 15% MnO_2. Significant tonnages of lower-grade silver and base-metal mineralization with relatively lower manganese content are found in surrounding stratiform and fracture zones (Table 1).

The main manganese oxide-rich zone forms a blanket-like body or manto up to 200 feet thick over a 2000 by 200 to 1000-foot area and is primarily confined to gently-dipping, Mesozoic pyroclastic and epiclastic tuffs of rhyolite composition. Texturally the manganese and minor iron oxides in the manto form crystalline veinlets, colliform and sooty encrustations which generally replace, fill open space, and are often apparently intergrown with jasperoidal and coarse-grained quartz that, in turn, had replaced the permeable, sandy horizons in the volcanics. Massive jasperoid continues in outcrop above the manganese oxide manto as a caprock and is also weakly mineralized. Other apparently similar, parallel, stratiform oxide zones above and marginal to the main manto crop out and contain similar mineral assemblages but also include relict sulfides.

Manganese oxide-rich mineralization, and silicification, locally extend for unknown distances into the underlying Permian limestones and sandstones (Figs. 5 & 6). In outcrop to the southwest of the main manto this mineralization is accompanied by jasperoid breccia and occurs along high-angle faults, fracture zones, and bedding planes in the Paleozoic section. In a broad sense much of the Hardshell mineralization appears to be stratiform, but high-angle fracturing and faulting, apparently related to district-scale structure, appear to exert strong control on the location, lateral extent, and concentration of mineralization within stratiform zones (Figs. 7, 8, 10).

This lateral control of mineralization by high-angle structure is particularly evident on structural contour and isopach maps which show that most mineralization is primarily confined to a series of pre-ore horst blocks which must have been active during volcanism. The most favorable horizon for mineralization is where Paleozoic rocks are immediately overlain by fine-grained epiclastic Mesozoic sandstones.

Other favorable horizons directly overlie or are marginal to major fracture or fault zones. Stop C examines the outcrop of one of these zones, the Hardshell incline. Unfortunately safety considerations and a plague of fleas preclude underground trips down the incline.

The main manto and Hardshell incline are well zoned (Figs. 8 & 9). A drill hole assay profile shows that the main manto-manganese-oxide-rich zone has distinct boundaries defined by a number of chemical elements, mineralogical and textural features. The upper part of the manganese oxide zone, the contained manganese oxides, and other ore minerals are Pb-rich, while the lower portion is Zn-rich. Sb shows close correlation with silver, while As is generally concentrated at the margins of the main manto, primarily as mimetite. Cu also closely follows silver and is also relatively high in the limestone root zones of the higher-grade portions of the manto. Manganese oxide is also generally higher in the lower portion of the manto.

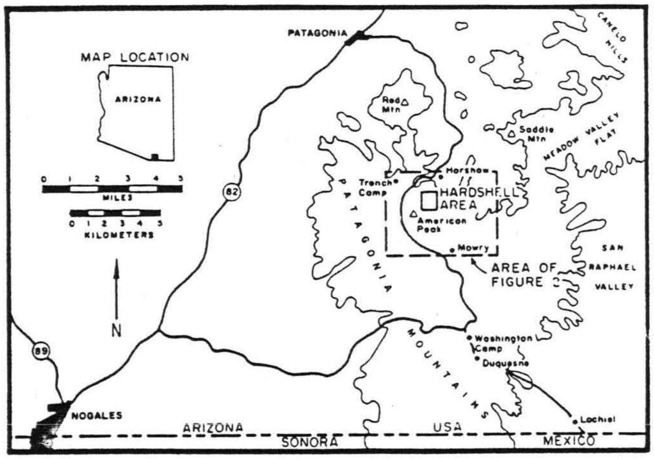

Figure 1. Location of the Patagonia Mountains (5000-ft. contour outline). The areas of Figure 2, the greater Hardshell area, and Figure 4, the immediate Hardshell area, are outlined.

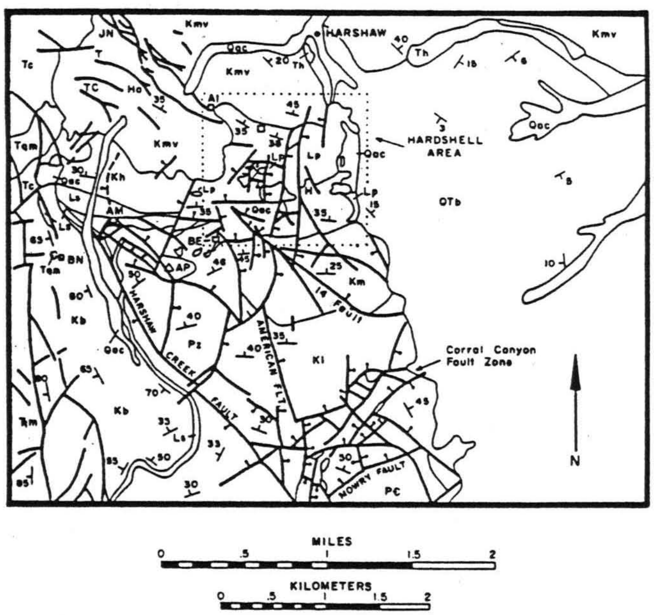

Figure 2. Geologic Map of the Greater Hardshell Area, Harshaw to Mowry, Northeastern Patagonia Mountains. Compiled from Davis (1970), ASARCO file data, Simons (1974) and Baker (1961).

EXPLANATION (Figure 2)

Q_{ac} Quaternary Alluvium and Colluvium.

QT_b Quaternary-Tertiary Basin-Fill Conglomerates, "Gila"-Type.

T_h Harshaw Tuffs, locally calcareous.

T_{qm} Quartz Monzonite Porphyry Intrusive.

T_c Chief Volcanics. (TK_v of Simons (1974)).

K_{mv} Trachyandesite of Meadow Valley. (Simons 1974).

K_h Hardshell Volcanics. Ash-Flow Tuffs and Breccias; Epiclastic Sediments.

lp Latite Porphyry Sills(?).

ls Limestone Conglomerate and Breccia.

K_m Lavas and Ash-Flow Tuffs.

K_l Volcanics and Sediments in Corral Canyon (Baker (1961); JTR_{vs} of Simons (1974)).

K_b Bisbee Group Sediments (Siltstones, Conglomerates, Limestones).

ls Limestone Marker Bed.

TR_m Mt. Wrightson Formation(?)-Simons (1974). Silicified Rhyolites, Tuffs, Quartzites.

Pz Paleozoic Sediments, Cambrian to Permian, Predominately Carbonates.

p€ Precambrian Quartz Monzonite and Hornblende Diorite.

s Massive Silica, Jasperoid, Jasperoid Breccia.

□ Shaft

35 Attitude of Bedding or Flow Foliation.

Fault- Ball and Bar on Downthrown Block.

ABBREVIATIONS

A-A	American Fault	BN	Blue Nose Mine
Al	Alta Mine	H	Hermosa Mine and Fault
Am	American Mine	JN	January-Norton Fault
AP	American Peak	M	Mowry Mine and Townsite
BE	Bender Mine	T	Trench (Hagen) Vein

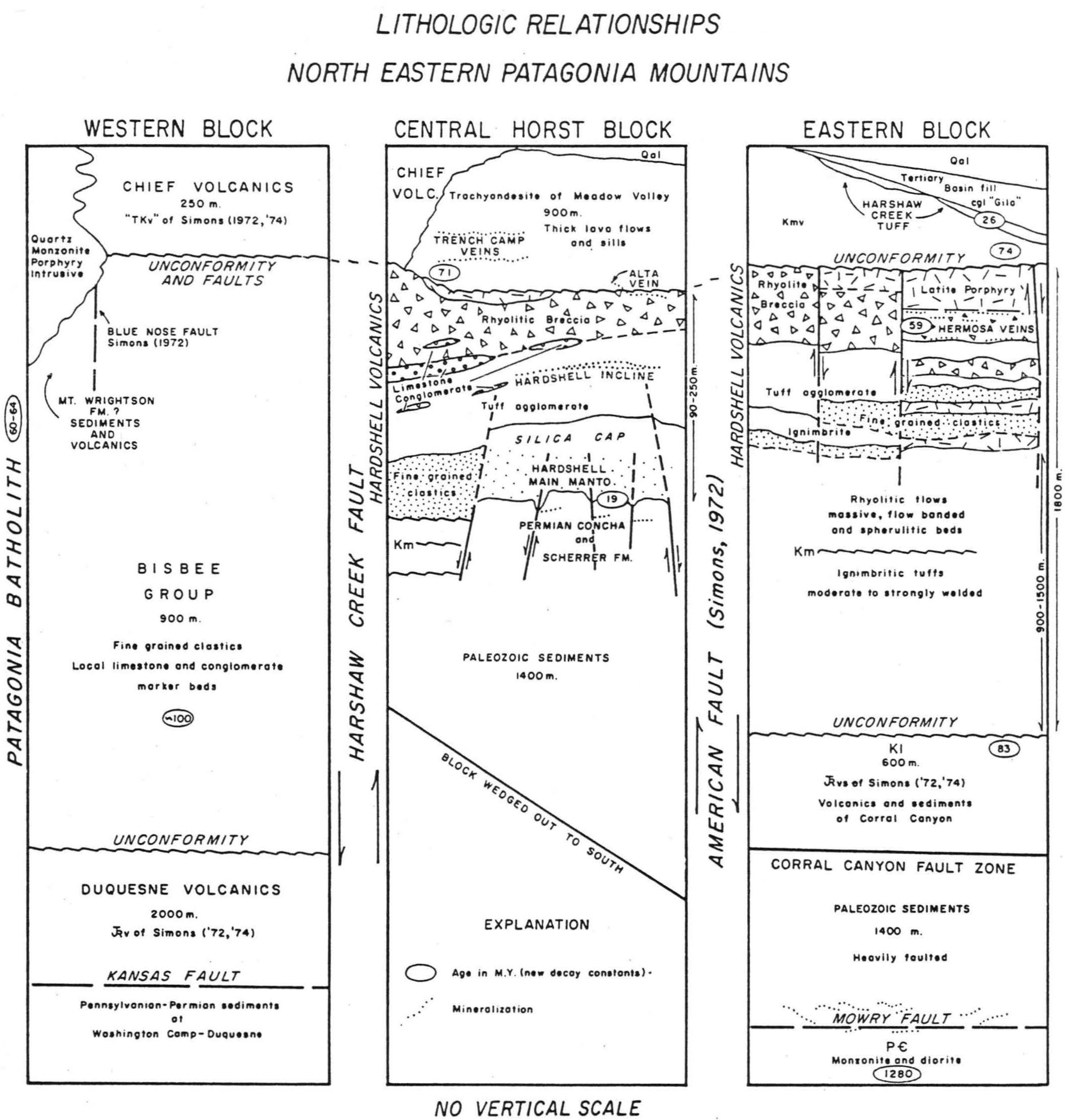

Figure 3. Lithologic Relationships and Tectonic Blocks, Northeastern Patagonia Mountains (in part, after Simons [1972]).

APPROXIMATE CHEMICAL COMPOSITION OF HARDSHELL ORE TYPES[1)]

	Main Manto Types			Other Stratiform Types		
	Pb/Zn > 1	Pb/Zn < 1	Massive Silica	Red Clay	Hermosa	Hardshell Incline
oz./T Ag	6.7	2.4	1	1.5	4	5.5
oz./T Au	0.008	0.005	-[2)]	-	-	0.008
% Pb	1.9	0.54	0.25	0.08	0.3	5.5
% Zn	0.44	1.8	0.02	0.01	0.05	2
% Cu	0.12	0.095	0.02	0.014	0.05	0.2
% Mn	8.0	12.4	0.25	0.06	2.	9.
% As	0.019	0.021	0.01	0.006	0.3	0.5
% Sb	0.134	0.068	0.05	0.02	2.	0.4
% Ba	0.15	0.01	0.01	0.05	0.015	0.015
% Cd	0.009	0.01	0.008	0.008	0.008	-
% Bi	0.005	0.005	0.005	0.005	0.005	0.02
% V	0.005	0.005	0.025	0.01	-	0.02
% CO_2	-	0.01-35.	-	-	-	-
% Sulfide	0.03	0.01	0.03	0.3	0.1	0.1
% Sulfate	0.02	0.04	0.05	0.1	0.2	0.1
% SiO_2	77	64(25-90)	94	74	70	55
% Al_2O_3	2	1.2	0.8	15	10	1-20
% Fe_2O_3[3)]	2.5	2	2.5	5	5	8
% MgO	0.05	0.15	0.01	0.2	0.2	-
% CaO	0.2	0.01-45.	0.02	0.02	0.1	0.5
% Na_2O	0.08	0.04	0.04	0.5	0.3	-
% K_2O	0.6	1.0	0.1	3.5	5.0	-
% TiO_2	0.02	0.006	0.006	0.15	-	-
Source of data	Drill	Drill	Drill	Drill	Drill & Production	Production & Underground Sampling

1) Estimates for ore types, this is not an ore reserve, amounts do not sum to 100% and not weighted for area of influence of drill holes and sampling.

2) - Means not analyzed.

3) Total iron as Fe_2O_3

Table 1.

HARDSHELL AREA MINERALOGY-IDENTIFIED

(lower case indicates of lesser importance)

Cryptomelane-Coronadite Group	$(K, Pb, Zn, Cu, Ag, Ba)(Mn^{+2}, Mn^{+4})_8O_{16}$
Romanechite Group	$(K, Pb, Zn, Cu, Ag, Ba)(Mn^{+2}, Mn^{+4})_8O_{16}(OH)_4$
Todorokite Group	$(Pb, Zn, Cu, Mn^{+2})Mn_3^{+4}O_7 \cdot H_2O$
Chalcophanite	$(Zn, Fe, Mn^{+2})Mn_3^{+4}O_7 \cdot 3H_2O$
Nsutite	$(X^{+2}, Mn_y^{+2})Mn_{1-y}^{+4}O_{2-2y}(OH)_{2y}$: y = small; X = Cation
birnesite	$(X, Na, Ca)Mn_7O_{14} \cdot 3H_2O$
Pyrolusite	MnO_2

Bromargyrite (Embolite) $Ag(Br, Cl)$
Acanthite Ag_2S
Galena PbS
Sphalerite $Zn(Mn, Fe)S$
Pyrite FeS_2
Covellite CuS
chalcocite Cu_2S
chalcopyrite $CuFeS_2$
native silver Ag
Cerussite $PbCO_3$
anglesite $PbSO_4$
Mimetite-Pyromorphite $Pb_5(AsO_4, PO_4)_3Cl$
descloizite-mottramite $Pb(Zn, Cu)VO_4(OH)$
vanadinite $Pb_5(VO_4)_3Cl$
wulfenite $PbMoO_4$
Willemite Zn_2SiO_4
bindheimite $Pb_2Sb_2O_6(O, OH)$
Tetrahedrite-Tennantite $(Cu, Fe, Zn, Pb, Ag)_{12}(Sb,As)_4S_{13}$
Jarosite $KFe_3(SO_4)_2(OH)_6$
Plumbojarosite $PbFe_3(SO_4)_2(OH)_6$
Alunite $KAl_3(SO_4)_2(OH)_6$
Hidalgoite-Beudanite $Pb(Al, Fe)_3(SO_4)(AsO_4)(OH)_6$
melanterite $FeSO_4 \cdot 7H_2O$
copiapite $(Fe, Mg)Fe_4^{+3}(SO_4)_6(OH)_2 \cdot 20H_2O$
Goethite $FeO(OH)$
Hematite Fe_2O_3
Magnetite Fe_3O_4
native copper Cu
cuprite Cu_2O
chrysocolla $Cu_2H_2Si_2O_5(OH)_4$
Malachite $Cu_2(CO_3)_3(OH)_2$
azurite $Cu_3(CO_3)_2(OH)_2$
brochantite $Cu_4(SO_4)(OH)_6$
atacamite $Cu_2Cl(OH)_3$
turquoise $CuAl_6(PO_4)_4(OH)_8 \cdot 5H_2O$
chenevixite $Cu_2(Fe, Al)_2(AsO_4)_2(OH)_4 \cdot H_2O$
chalcanthite $CuSO_4 \cdot 5H_2O$
barite $BaSO_4$
sphene $CaTiSiO_5$
apatite $Ca_5(PO_4)_3(F, OH, Cl)$
zircon $ZrSiO_4$
Gypsum $CaSO_4 \cdot 2H_2O$
Calcite $CaCO_3$
Mn-Calcite $Ca(Mn)CO_3$
Rhodochrosite $MnCO_3$
siderite $FeCO_3$
ankerite $Ca(Fe, Mg, Mn)(CO_3)_2$

Sericite (illite) $KAl_2Si_3O_{10}(OH)_2$
Montmorillinite Group (including Saponite-Sauconite) $(Ca/_2, Na)_{0.33}(Mg, Fe, Zn)_3(Si, Al)_4O_{10} \cdot 4H_2O$
Kaolinite $Al_2SiO_5(OH)_4$
"Allophane" $Al_2SiO_5 \cdot nH_2O$
Quartz SiO_2
Sanadine)
Orthoclase) $KAlSi_3O_8$
Microcline)
"Adularia")
Plagioclase $NaAlSi_3O_8-CaAl_2Si_2O_8$
Chlorite $(Mg, Fe^{+3}, Fe^{+2}, Mn)(AlSi_3)O_{10}(OH)_8$
Epidote $Ca_2(Al, Fe^{+3})(SiO_4)_3(OH)$
Biotite $K(Fe, Mg)_3AlSi_3O_{10}(F, Cl, OH)_2$

Table 2.

The top of the MnOxide zone often has a strong silver "kick," suggesting possible supergene enrichment.

The lower portion of the massive silica caprock has a distinctive greasy-green color — caused in part by the oxidation products of sulfides. Increased percentages of clear, coarse-grained quartz veinlets also indicate nearness to main manto mineralization. In the main manto and incline the percentage of coarse-grained, zoned, often terminated, quartz crystals closely correlates with grade of mineralization.

The top of the massive silica is defined by a red "clay" zone with increased percentages of sericite and kaolinite with hematite and goethite after pyrite. The red clay zone is anomalous in silver, copper, and antimony. The altered volcanics over the massive silica are characterized by iron oxides after mainly pyrite, by sericite-illite with local montmorillonite and, distinctively, by rhombic K-feldspar or adularia. Adularia preferentially replaces pumiceous and fracture zones in the Hardshell volcanics and is an excellent guide to bonanza silver halide mineralization at the Hermosa mine (Figs. 4 & 5b) on the SE end of Hardshell Ridge. Outward from adularia-quartz filled fractures one or more clay-sericite zones are present in stockwork-fractured areas. The K_2O zoned enrichment (and Na_2O depletion) of already alkali-rich rocks is particularly evident on chemical profiles of drill holes over the main manto.

Other guides to mineralization in the Hardshell area include alunite veins, sulfidation of magnetite in the volcanics, an iron oxide color anomaly from the oxidation of pyrite, manganese oxide dendrites, and increased fracturing.

Besides the main manto, there are other stratiform Mn-oxide-rich zones, the most developed of which is the Hardshell incline (Figs. 5a & 10). The Hardshell incline has similar Pb-Zn-Mn zoning to the main manto, but has much better defined structural as well as stratigraphic control to the zoning.

The present preferred origin of the silver, base-metal manganese oxides is <u>in situ</u> oxidation, with only minor supergene transport, of a primary assemblage containing manganese sulfide (alabandite) and carbonates, galena, sphalerite, pyrite, chalcopyrite, and silver-bearing sulfosalts similar to that at the Alta and Trench Camp mines. Much of the evidence for the origin of the manganese oxides comes from subsurface data and laboratory studies including detailed mineralogical identification of textures, phases and compositions, metal zoning, isotopic age dating, and fluid inclusion work.

Figure 11 shows some of the manganese oxide mineral structures found at Hardshell — the most common of which is the hollandite group. The hollandite group includes a wide variety of solid solution end members — specifically at Hardshell: cryptomelane-coronadite in which K^+ and Pb^{+2} are contained in the tunnel site of the structure: XMn_8O_{16}. A wide variety of other large cations including Ag^+ also substitute in this site. Recent work has shown that the manganese oxide groups are quite complex and may even be interlayered similar to the illite-montmorillonites. Other important silver-bearing minerals in the Hardshell area are acanthite and silver halides. Table 2 lists all minerals that have been specifically identified from the Hardshell area.

Figure 12 shows fluid inclusion homogenization and freezing temperatures from the Hardshell area. Main stage (pre-manganese oxide) quartz, calcite, and sphalerite range from 400° down to 240°C, uncorrected for pressure, with relatively low salinities. Late-stage (post-Mn oxide) calcite, quartz, and cerussite range from about 180°C down to less than 40°C with very low salinities. These temperatures and salinities with the presence of vapor-rich fluid inclusions above about 340°C would suggest a depth of formation of 1.5-2.0 km in a hydrostatic system. For comparison, stratigraphic evidence suggests at least 1 km of cover over the Hardshell deposit during hypogene mineralization. Evidence suggests that boiling and temperature fluctuations were cyclic and that several horizons, particularly the "red clay"-zone at the top of the massive silica were horizons of boiling.

Main stage quartz and calcite prior to manganese oxides have similar fluid inclusion temperatures to main stage quartz and sphalerite intergrown with other sulfides. This suggests that the manganese oxides are secondary products of previous minerals. A second thermal event would account for the relatively high post-Mn oxide temperatures.

Support for two distinct thermal events comes from K/Ar dates (Fig. 3) on Hermosa adularia (59 m.y.) formed at about 270°C and on cryptomelane (19 m.y.) from the base of the main manto. The date on the cryptomelane does not suggest the age of the second thermal event, but the 29 and 24 m.y. ages on the Harshaw Tuff suggest that volcanism was active in the Mid-Tertiary. Additional support for Mid-Tertiary oxidation at Hardshell comes from the presence of Hardshell-type manganese-oxide-jasperoid boulders in the "Whitetail-Gila"-type basin-fill conglomerates above the Harshaw Tuff in the headwaters of Harshaw Creek.

FIELD TRIP STOPS

NOTE: From a vantage point on the saddle of Red Mountain, several important tectonic, physiographic, and geologic features were pointed out on the morning portion of the original field trip. These included the main range of the Patagonia Mountains, NW-trending Alum Gulch controlled by the January-Norton shear zone, the dumps and tailings at the Worlds Fair and Trench Camp mines, Harshaw townsite and Creek, American Peak (45° N-dipping, Permian carbonates and sandstones armored by jasperoid breccias on the summit), Hardshell Creek, drill roads and the faint iron oxide color anomaly on Hardshell Ridge, Hermosa Canyon, the San Rafael Valley, and the Late Tertiary conglomerates being dissected by the headwaters of Harshaw Creek. A brief discussion of circular linear features, possible calderas, and zones of major NW faulting also took place from this vantage point.

<u>STOP A:</u> (Lunch-site) <u>Harshaw Townsite.</u> Harshaw had approximately 2000 people in the immediate area 100 years ago, mostly associated with the Hermosa mine and mill, the Trench Camp mines and a wide variety of prospects in the local area. Harshaw was relatively active up until the late 1960's when much of the townsite was cleared by the U. S. Forest Service. The ASARCO Trench Mill on the hill to the west operated from 1939 to 1964 treating ores from the Trench Camp veins, the Flux mine and custom ores from the Washington Camp-Duquesne area.

Around the Harshaw townsite the thick flows of the basal trachyandesite of Meadow Valley (Simons, 1972) called "diabase" in ASARCO field terminology and the overlying white, biotitic Harshaw Tuff of air-fall and water-laid origin can be noted.

An interesting contact in the trachyandesite can be observed on the cliffs above the Harshaw cemetery. A latitic horizon at a flow contact in the trachyandesite contains blocks of andesite and vice-versa. Such latitic horizons are common in the trachyandesite with a pink groundmass of K-feldspar and finely divided hematite. Amygdaloidal flow-top horizons with strong hematite and alteration are common in the Harshaw area and were a good guide to ore. Ore shoots developed where the fissure-veins (January-Norton shear zone) of the Trench Camp mines intersected the slightly shallower-dipping trachyandesite flow-tops.

Travel 0.9 mile SW on the Harshaw Creek road to Hardshell Camp. One adobe building remains east of the road. Turn left (east) and proceed about 1200 ft. to the dumps at the Alta Mine. Note how the "diabase" weathers to cobbles.

STOP B: (Park trucks; proceed on foot from here) Alta Mine Dumps. The Alta vein dips about 40° NNE and was essentially stratiform within the Hardshell rhyolite breccia. The rhyolite is overlain in slight angular unconformity by the trachyandesite. An amygdaloidal-hematitic shear zone in the trachyandesite can be traced to the NW into elements of the January-Norton shear zone. Shrader (1915) reported that the Alta vein was 2-3 ft. wide and extended to about 300 ft., but the works had been dismantled by 1905. Production was 3500 tons 35% Pb, 1% Cu, and 10 oz. Ag/T with minor Au (Keith, 1975). A wide variety of sulfides and their oxidation products can be noted in the jarositic dump material including galena, sphalerite with various amounts of Fe and Mn, chalcopyrite, tetrahedrite, pyrite, rhodochrosite. Under the microscope, covellite, acanthite, ruby silvers, and embolite can also be noted.

Proceeding up Hardshell Creek, the 30-40° NE dip of the Hardshell rhyolite breccia is obvious. The Mn and Fe oxide staining on shears in the stream cut dies to the SE. Unfortunately the bed of Hardshell Creek is covered with alluvial and reworked dump material from flash floods which covers the trace of the Hogan fault zone (continuous with the Alta and January-Norton fault systems). The creek bed provides a wide variety of mineralization types from mines upstream.

No actual offset on the Hogan fault zone more than a few feet of reverse movement can be demonstrated. However, the juxtaposition of NE-dipping rhyolite to the NE and the similar-dipping trachyandesite flows to the SW suggests some offset. An unconformity and topography on the top of the rhyolite may account for some of the apparent offset. The dumps of the Hardshell incline and tailings from the oxide mill can be noted along the left side of the canyon. The airshaft of the Hardshell incline is on the left.

STOP C: Hardshell Incline - dumps at the old Engine Room (Incline portal is caved). The Hardshell incline area was first staked in 1879, but the incline zone was not discovered until 1895 when R. R. Richardson sunk a 40' vertical shaft and ran the incline to 230 level. From 1896-1905 the incline was extended to the 500 level and about 20,000 tons of shipping and milling ore were mined. Sporadic mining from 1905 to 1940 produced several thousand tons of ore including Mn ores during WW I. ASARCO optioned the mine in 1940 in search of sulfide ores to feed the Trench mill. The sulfide ore search was unsuccessful, but about 2500 tons of oxide Pb-Ag ore was produced from 1943-1948. In 1963-64 McFarland, also leasing the Trench mill and Flux mine, produced about 2900 tons of oxide Pb-Ag ore, mostly from below the 500 level. Production has averaged 6% Pb and 8 oz. Ag/T.

In the late 1940's and early 1950's drilling for sulfide ores around the incline led to the discovery of Mn-oxide-Ag mineralization at the Paleozoic/volcanic contact (Fig. 5a). The major drilling project, about 45 holes, that delineated the main manto took place in 1967-68.

The Hardshell incline develops a series of 25-40° north-dipping stratiform zones from a few up to 40 feet thick. The mineralized horizons are arranged in a NE-plunging en echelon fashion and are limited laterally (Fig. 10) by high-angle, NE-dipping shears parallel to the Hogan zone. Much of the mineralization replaces sandy epiclastic and air-fall tuffaceous zones in the generally well-welded tuffaceous agglomerate. Locally, stockwork-like fractured masses within the more competent, welded units are well altered and mineralized. Argillic/illitic alteration — primarily montmorillonite and kaolinite zones, in and around mineralization up to 50 feet thick, are developed and are locally sheared by post-ore movement along bedding planes. Some bedding plane movement and brecciation are pre-ore.

Two main ore types occur in the incline. Footwall ores are Mn-Ag-Zn>Pb-rich and are very similar to main manto ores. Hanging-wall Pb-Ag ores are manganese and zinc-poor (and often iron-rich) and essentially consist of cerussite with minor anglesite, galena, and pyromorphite-mimetite. The dump material contains these and a wide variety of oxidized Pb, Zn, Cu, Mn, Fe, Ag, As and Sb minerals listed on Table 2.

Structural contours on the top of massive silica and the manganese-oxide manto underlying the incline show an antiformal surface over the Hogan fault zone, suggesting NW fracture control of mineralization along Hardshell Creek (Figs. 7 & 8).

STOP D. Stream cut across from Hardshell incline dumps. Hardshell Creek has scoured to bedrock here exposing a volcanic conglomerate with a wide variety of well-rounded clasts in a tuffaceous matrix. Some NW-trending Fe and Mn-oxide filled fractures can also be noted here. The general N to NE dip of the volcanic section, minor flexure of the beds, and high angle faults (some apparently post-mineral) are evident in the immediate area. The volcanics in the stream cut were mapped by Davis (1970) as part of tuffaceous agglomerate/conglomerate unit of the Hardshell (formerly Chief) Volcanics. Actual lithologic units of the Hardshell Volcanics are difficult to trace both laterally and vertically outside the area of close-spaced drilling. Your opinion on the volcanic environment represented by the various units in the Hardshell area is invited. Many have suggested, and I believe, that this is a caldron-margin environment with mega- and meso-breccias.

Proceeding up Hardshell Creek the massive silica caprock can be noted on the canyon walls to the south and east. Minor old workings are located along high-angle fracture zones and thin stratiform zones south

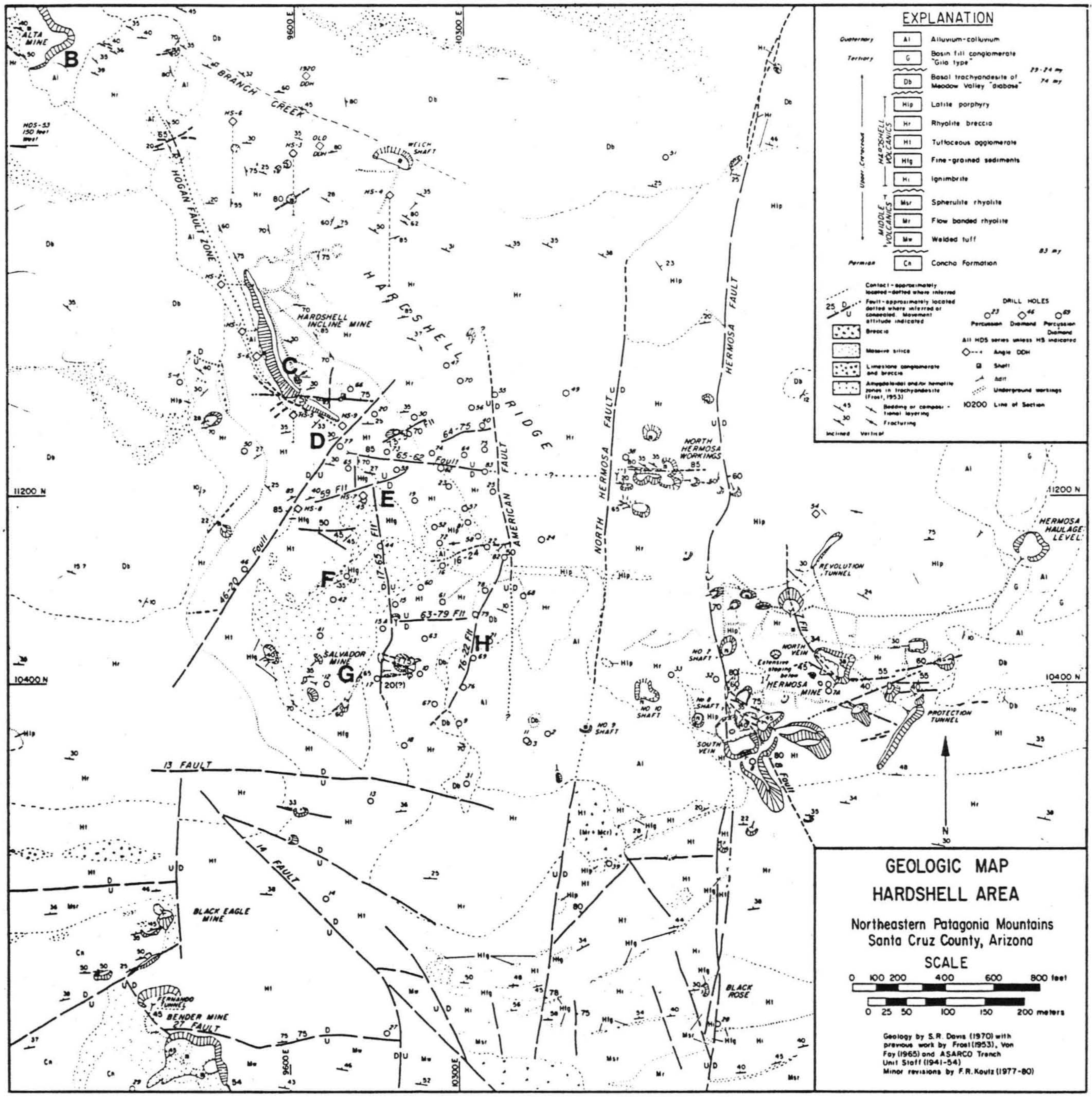

Figure 4. Geologic map of the Hardshell area. Stops B through G involve a walk from the Alta Mine dumps (in the NW corner) up to the Hogan fault zone to the southeast with major stops at the Hardshell Incline, Ht-Hfg contacts, limestone breccia and conglomerate west of the 17-65 fault, in the massive silica caprock and at the outcrop of the main manto orebody at the Salvador Mine. Stop H examines the diabase-rhyolite breccia contacts and alteration in the rhyolite along drill roads on Hardshell Ridge.

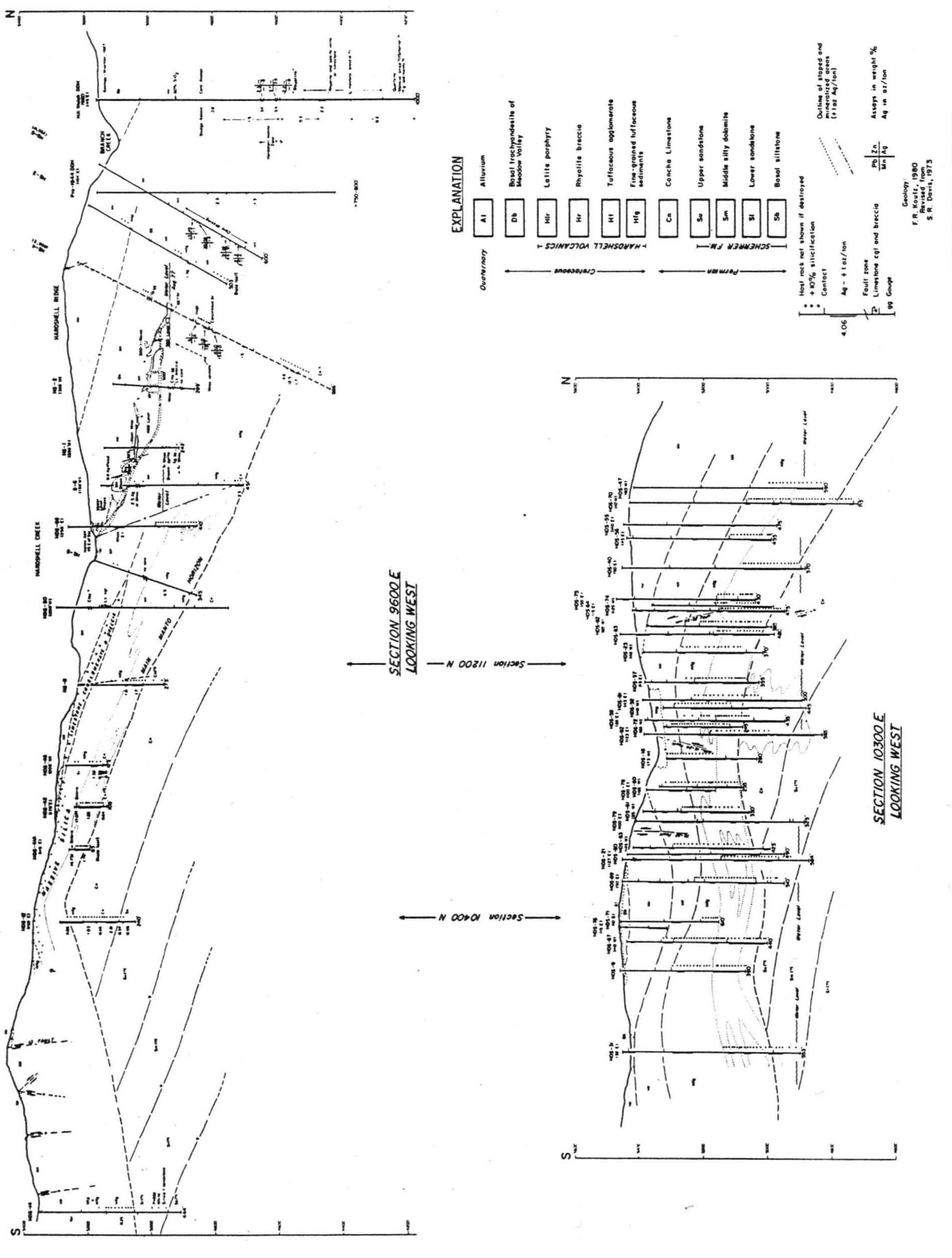

Figure 5a. N-S cross-sections looking west, Hardshell Deposit. Note positions of main manto and Hardshell Incline.

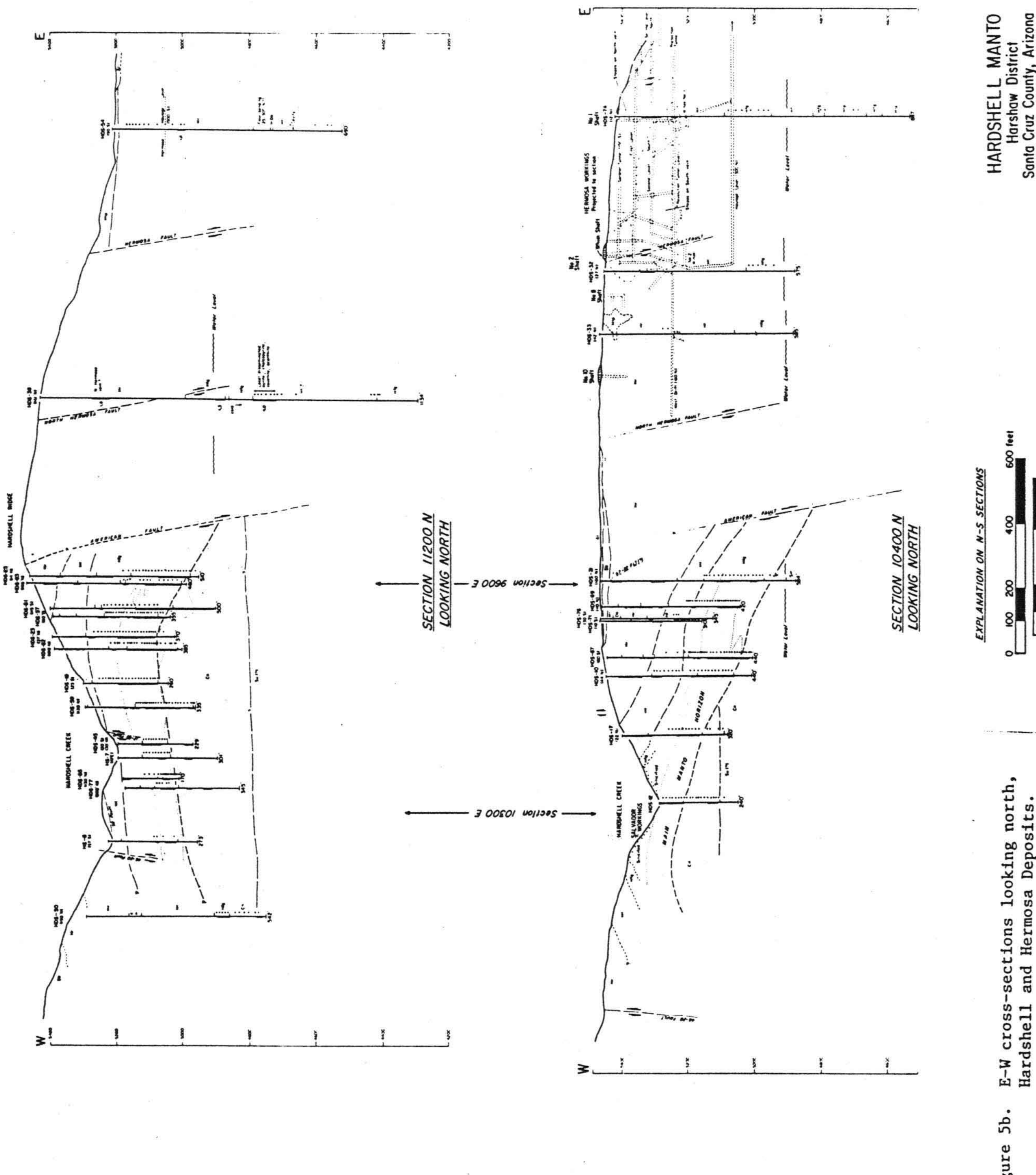

Figure 5b. E-W cross-sections looking north, Hardshell and Hermosa Deposits. Note position of water table.

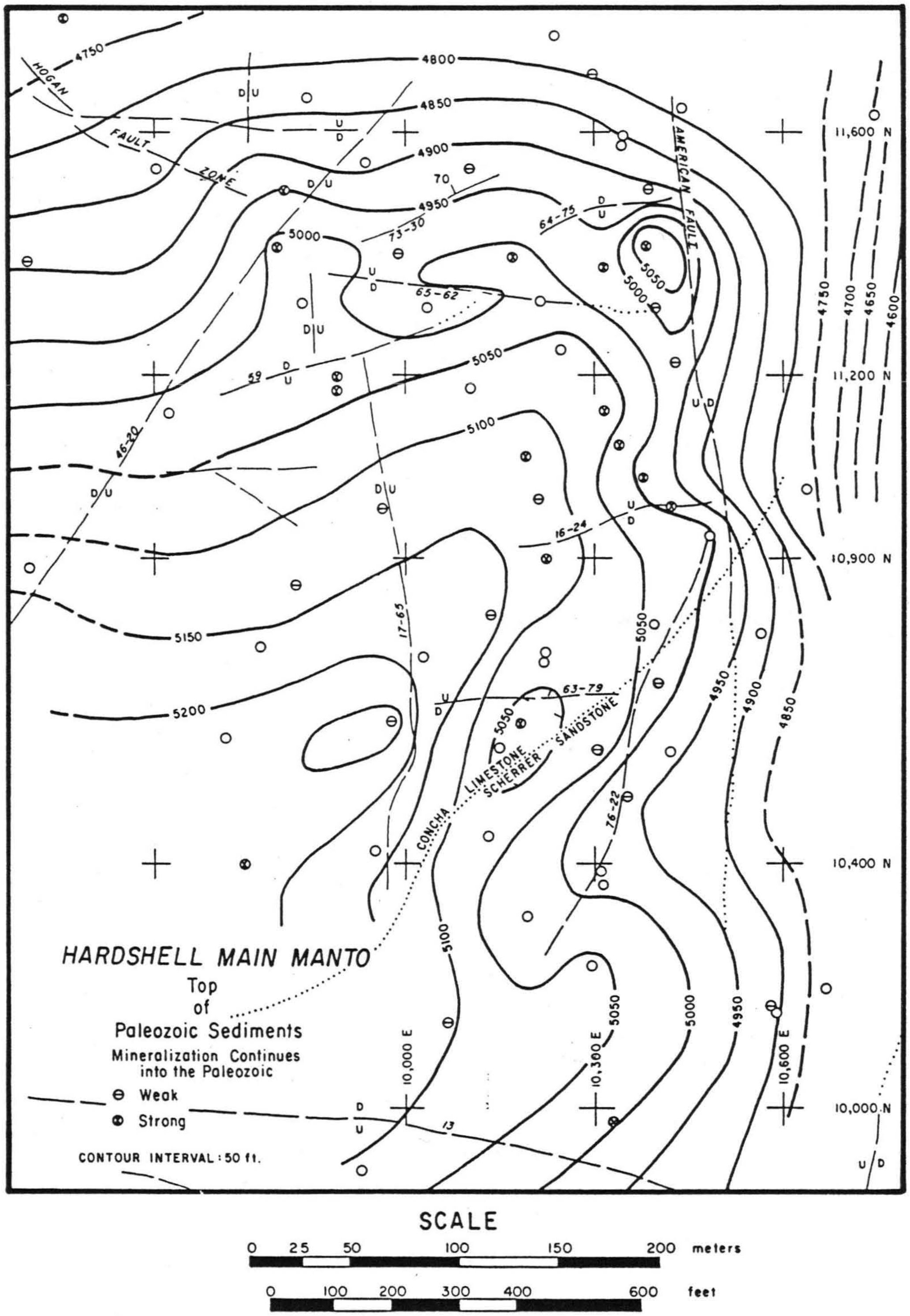

Figure 6. Structure contours on top of Paleozoic. Fault traces are on the outcrop surface and not projected to the Paleozoic.

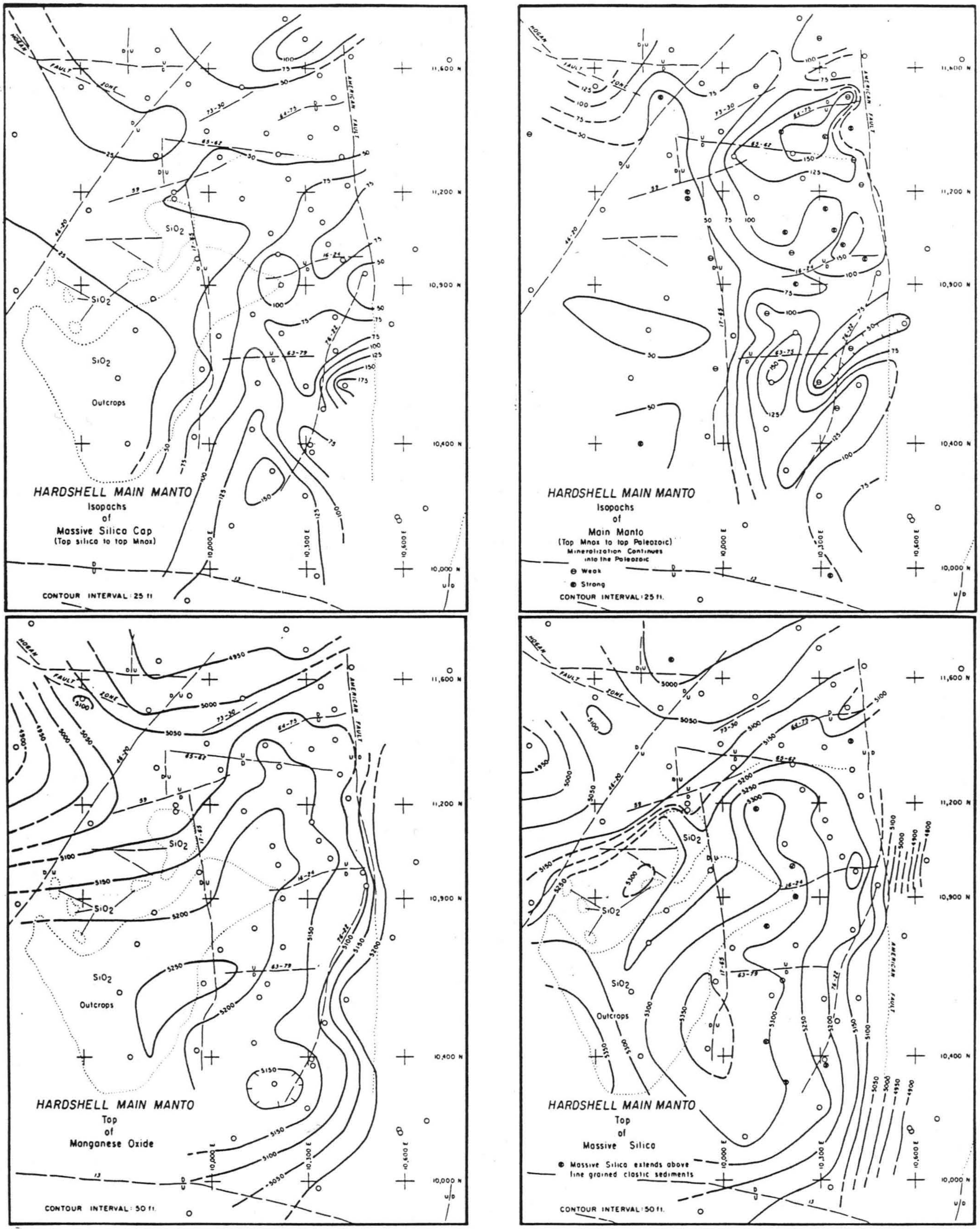

(Grid Scale in Feet)

Figure 7.

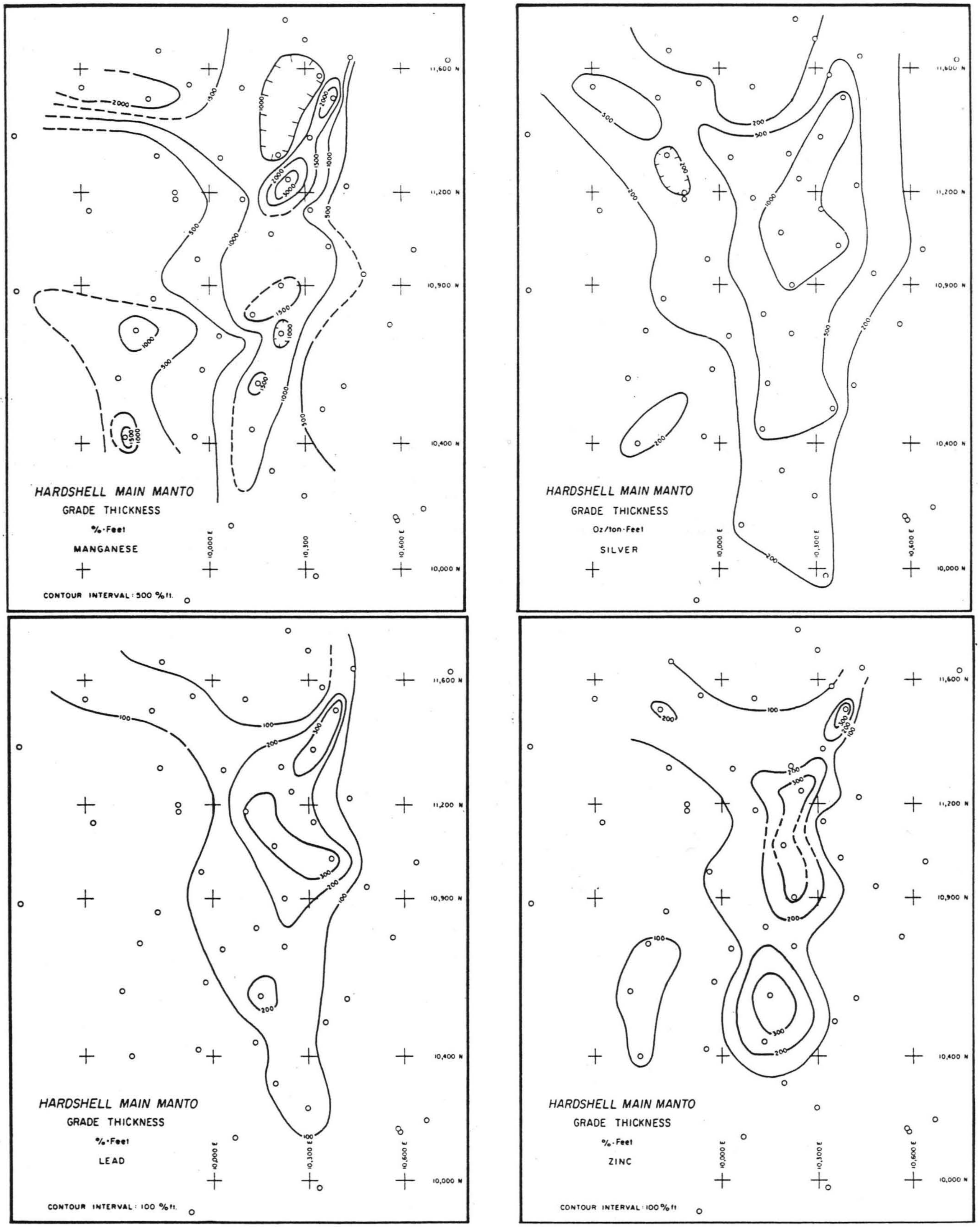

(Grid Scale in Feet)

Figure 8.

of the incline along the east side of the canyon. Mineralization was primarily Mn-oxides or silver halides associated with adularia and quartz-filled fractures. Only a few of the workings produced more than 100 tons. A wide variety of jasperoid-Mn-oxide textures can be noted in the boulders in the creek bed.

STOP E. Outcrop of unsilicified fine-grained clastic unit (ore host) of the Hardshell Volcanics. This is at the gradational contact zone with the overlying tuffaceous agglomerate unit. Beds containing breccia fragments are not uncommon in the fine-grained unit. Strong Liesegang banding after disseminated pyrite in tuffaceous matrix is common. Elsewhere the fine-grained unit exhibits fluvial cross-bedding. Most of the fine-grained tuffaceous sandstone has been replaced by fine-grained, jasperoidal silica along Hardshell Creek, but the breccia horizons are still locally visible. Proceed up Hardshell Creek noting strong lateral as well as vertical control of silicification/mineralization and the wide variety of altered/mineralized boulders in the creek bed.

STOP F. Outcrop of limestone conglomerate unit of Hardshell Volcanics along west side of Hardshell Canyon. Breccia clasts and cobbles of Paleozoic limestone, mostly from the Permian Concha and Scherrer Formations are locally common in the Hardshell Volcanics and are often found throughout the Mesozoic volcanic section of SE Arizona (Simons and others, 1966). Beds containing cobbles, usually less than a foot in diameter are most common, but blocks up to several hundred feet long and tens of feet thick can be noted. Limestone conglomerates are most common at or near unconformities in the volcanic section, for example, along the Hardshell incline horizon.

The limestone clasts or cobbles generally make up 70 to 95% of the unit. The matrix consists of well silicified and altered, sometimes welded, volcanics similar to the tuff agglomerate and rhyolite breccia units. The limestone unit as a whole and many of the fragments are locally brecciated, rehealed, and silicified, especially near upper and lower contacts. Higher proportions of volcanic fragments are found near the contacts and often the unit appears to be completely gradational into the enclosing volcanics. The limestone clasts are often marmorized and replaced by fine-grained silica with trace wollastonite. In northwest Alum Gulch at the Flux mine, these limestone blocks in volcanics are mineralized.

The limestone breccias and conglomerates have been well described by Simons and others (1966) and Davis (1970). Possible modes of origin supported by field evidence include fluvial action, landslide-gravity slide blocks, lahars, rafting or dragging by lava, ash or breccia flows or as xenoliths in an eruptive breccia.

Proceeding up Hardshell Canyon down through the jasperoid caprock to the main manto, the canyon narrows. A wide variety of relict textures (including breccia clasts and chert nodules) in the jasperoid can be noted. As the Salvador mine is approached, increased percentages of greasy yellow-green flooding can be noted in the jasperoid, probably caused by finely divided minerals of the jarosite-iron sulfate group. Microscopically the jasperoid becomes coarser grained. The percentage of clear and cloudy quartz veinlets cutting the jasperoid increases and the width of the veinlets increases. All the rock here and in the stream bed is "ore" running in excess of 5 oz. Ag/T.

STOP G. Salvador Mine. This area is the closest outcrop to the upper surface of the main manto and represents leakage of manganese oxide mineralization. The southwestern edge of the main manto is only a few tens of feet below. The most prominent fracturing is E-W, dipping about 35° N and is on trend with fracturing in the Hermosa mine about 2500 feet to the east. Here as elsewhere at Hardshell, low-angle fracturing and shearing may reflect old bedding planes.

About 1000 tons of 30 oz. Ag/T ore were shipped in the 1880's and 2800 tons of 20 oz. Ag/T (2% Pb, 2% Zn, 15% Mn) ore were shipped from 1936-1944. Careful examination of fractures in the Salvador works will reveal drusy quartz-lined vugs with Mn-oxide encrustations and needles, identical to main manto ores intersected in drilling. Trace amounts of pyromorphite-mimetite and cerussite can also be noted.

Farther up the canyon the Black Eagle and Bender mines contain similar mineralization along high-angle fractures and faults between Paleozoic limestones and Hardshell Volcanics and short distances along bedding planes. These faults localized silicification producing jasperoids and jasperoid breccia. Such structures are similar to those beneath the main manto.

Proceed back down Hardshell Canyon to the Alta Mine to pick up vehicles and re-examine the section. Drive up the Branch Creek road past the Welch Shaft sunk in 1920 to 420 ft. in hopes of encountering Hardshell incline mineralization at depth. High inflows of water prevented extensive development on the 420 level, but fault gouge containing thin stringers of galena and the usual oxidized Hardshell assemblages were encountered. The Welch Shaft served as a water supply to the Trench mill from 1939-1964.

Proceed uphill to the SE crossing a sill or flow of latite porphyry in the Hardshell Rhyolite Breccia and the North Hermosa workings at about 5400' elevation. Note that the plateau along Hardshell Ridge can be projected across to the San Rafael Valley to the east. This area of Hardshell Ridge was probably only thinly covered in Mid-Tertiary time and locally has deep soil development.

STOP H. Park trucks and proceed on foot on drill roads. Thin outliers of "diabase" exposed here are slightly more porphyritic than upper parts of the trachyandesite. This led Simons (1974) to suggest that these outliers were actually apophyses of a pyroxene monzonite pluton feeding trachyandesite flows. Drilling shows this to be wrong, although a few thin dikes of trachyandesite have been encountered at depth.

Some of the high-angle fracture zones and textures in the rhyolite breccias can be examined along the drill roads. Many of the fracture zones are flooded with adularia and quartz; others have a distinct orange jarositic-hematitic gouge zone. The exact trace of the American fault against which the main manto terminates is not exposed, but is well defined by drilling. Although many of the north-south, east-side down faults in the area have minor post-mineral movement, most of the movement must be pre-trachyandesite since trachyandesite shows only

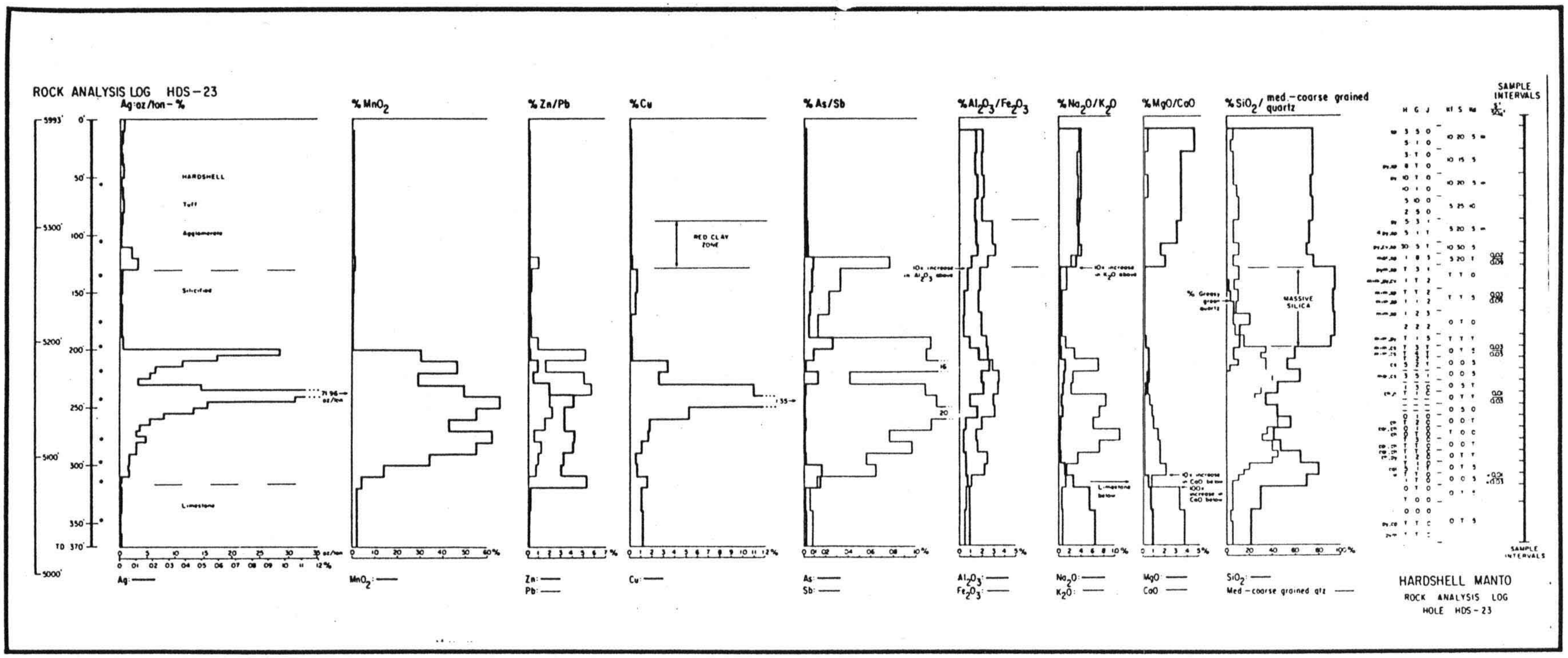

Figure 9. Rock analysis log through one of the higher-grade drill holes through the main manto. Note the positions of change in scale of Al 0 , K 0 and CaO.

Abbreviations: H = Hematite, G = Goethite, J = Jarosite, Kf = Potassium-feldspar, S = Sericite, Ka = Kaolinite, m = montmorillonite, py = pyrite, sp = specularite, mal = malachite, cv = covellite, pym = pyromorphite, mim = mimetite, cs = cerussite, ch = chalcophanite, n = nsutite, cal = calcite (late veinlets), w = willemite, cp = chalcopyrite. Mineral estimates in volume percent; less than 1% unless indicated. H & G percentages with dot to right indicate percent of drill chips strongly flooded with hematite or goethite.

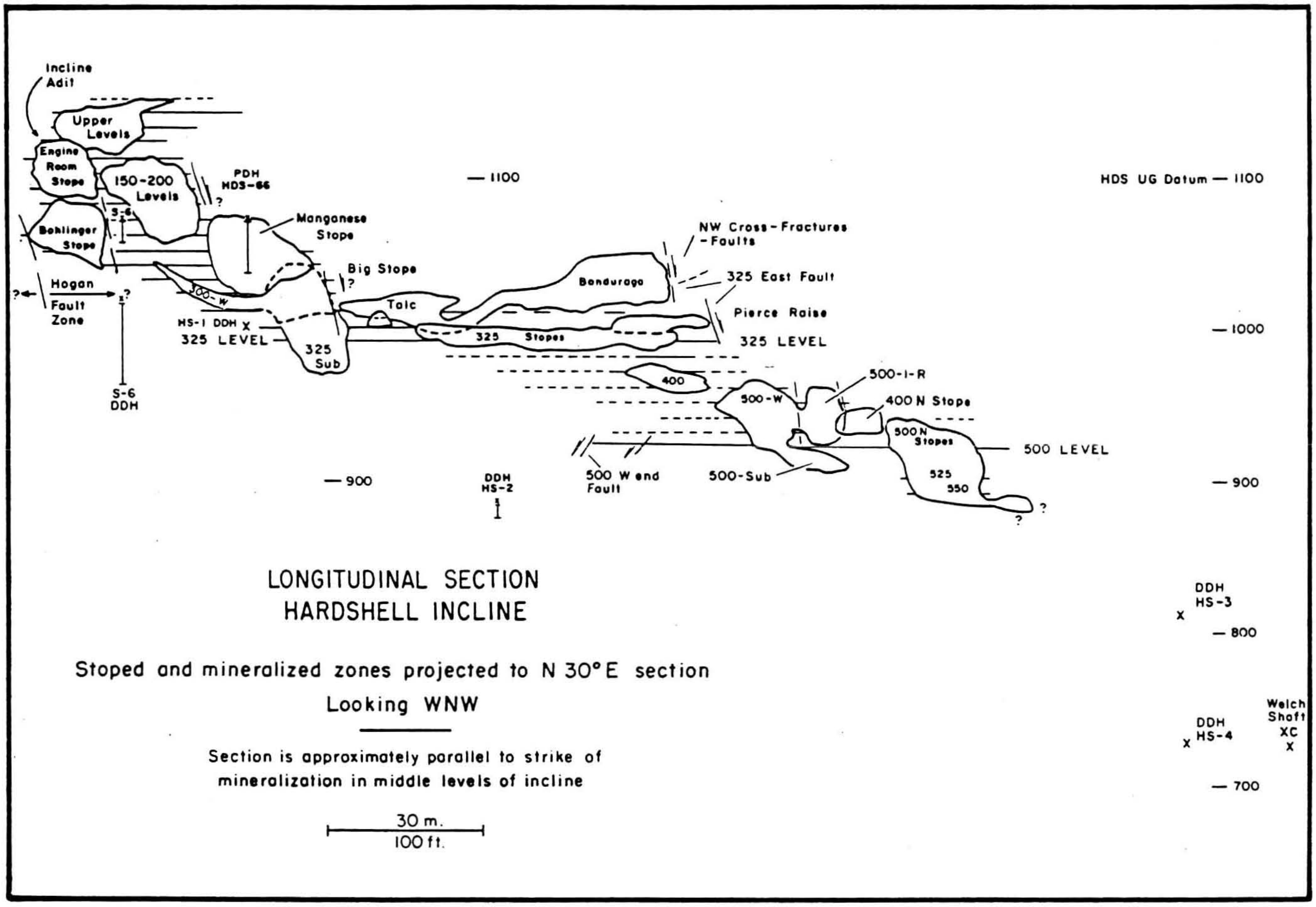
Incline Adit
Upper Levels
Engine Room Stope
150-200 Levels
PDH HDS-66
Bohlinger Stope
Manganese Stope
Big Stope
Hogan Fault Zone
HS-1 DDH
325 LEVEL
325 Sub
S-6 DDH
Talc
325 Stopes
Bandurraga
NW Cross-Fractures - Faults
325 East Fault
Pierce Raise
325 LEVEL
400
500-W
500-1-R
400 N Stope
500 N Stopes
500 LEVEL
500 W end Fault
500-Sub
525
550
DDH HS-2
— 1100
HDS UG Datum — 1100
— 1000
— 900
— 900
DDH HS-3
— 800
DDH HS-4
Welch Shaft XC
— 700
LONGITUDINAL SECTION
HARDSHELL INCLINE
Stoped and mineralized zones projected to N 30° E section
Looking WNW
Section is approximately parallel to strike of mineralization in middle levels of incline
30 m.
100 ft.

Figure 10.

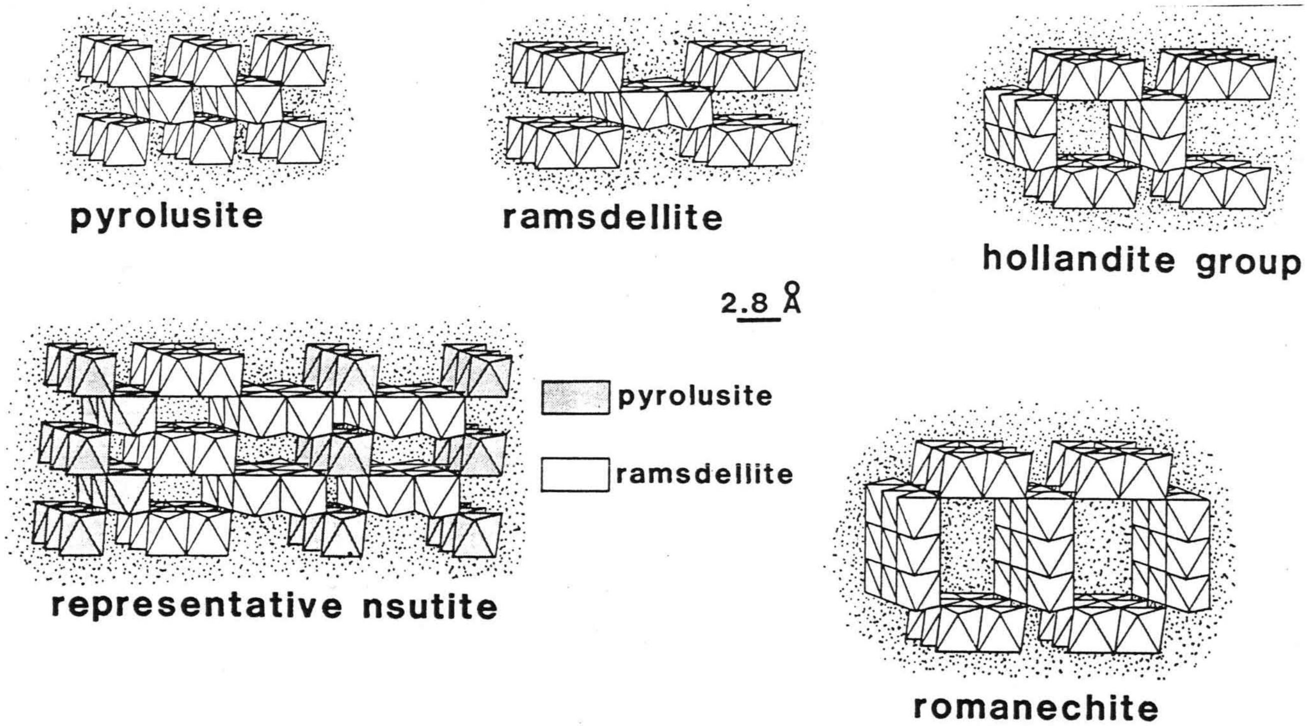

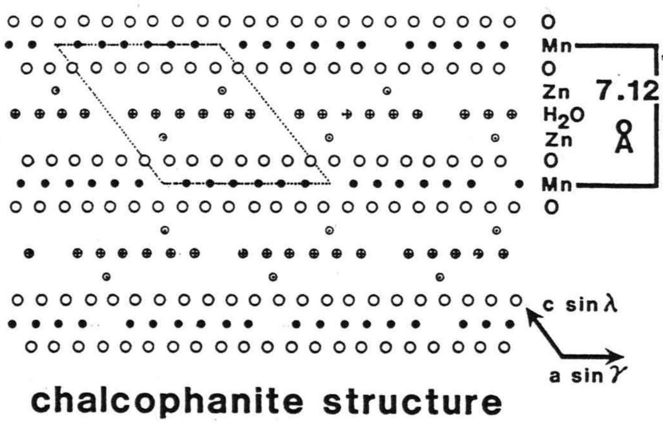

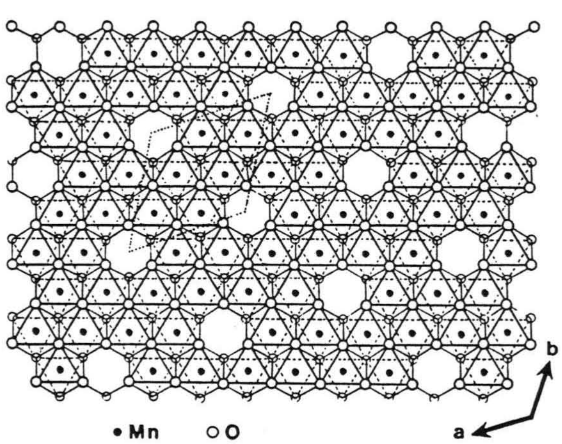

Ag^{+}	= 1.26	Mn^{++}	= 0.80
Au^{+}	= 1.37	Mn^{+4}	= 0.60
Ba^{++}	= 1.35	Fe^{++}	= 0.76
K^{+}	= 1.33	Fe^{+3}	= 0.64
Pb^{++}	= 1.20	Zn^{++}	= 0.74
Sr^{++}	= 1.13	Ti^{++}	= 0.90
Ca^{++}	= 0.99	V^{+3}	= 0.74
Na^{+}	= 0.95	Sb^{+5}	= 0.62
Cu^{+}	= 0.96	As^{+5}	= 0.47
Cu^{++}	= 0.69	Al^{+3}	= 0.50
Mg^{++}	= 0.65	Si^{+4}	= 0.41
		$S^{=}$	= 1.84
Ionic Radii in Å		Ar^{0}	= 1.74

Figure 11. Manganese Oxide Mineral Structures (after Burns and Burns, 1977). Hollandite and romanechite groups usually include large cations such as Ba, K, Pb, Ag, Na, or H_2O in tunnel-sites which hold the structure open. Pyrolusite, ramsdellite and nsutite generally form where large cations are not available. Ag may substitute for Zn in the layered chalcophanite structure.

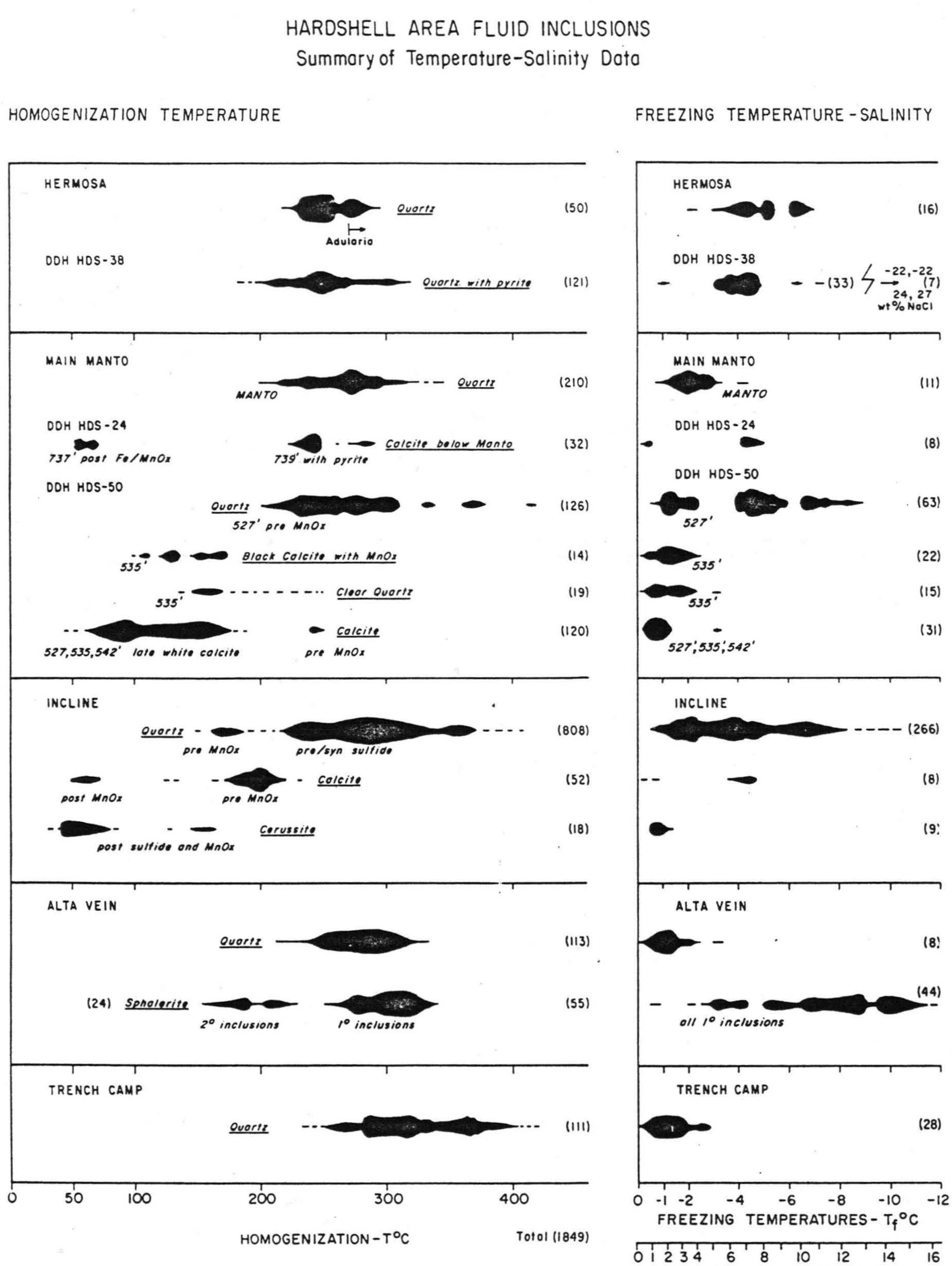

Number of inclusions in parentheses
Width of symbols proportional to frequency - normalized for each locality
Temporal relations between sample localities not implied nor intended
Sample localities listed east (top) to west (bottom)

Figure 12.

minor offset. The majority of fault offset may be synchronous with volcanism since volcanic units abruptly thicken and repeat themselves to the east of these faults (Fib. 5b).

These north-south high-angle faults must have strongly limited mineralization to the east since the favorable fine-grained clastic units in the Hardshell Volcanics are only weakly mineralized except for thin zones like the Hermosa Mine. Depth to the Paleozoic in the Hermosa area is in excess of 1200 ft. and could be up to 7-8000 ft., based on the Mesozoic section exposed between Hermosa and Mowry (Figs. 4 & 5b).

In summary, most Hardshell mineralization is localized in a series of horst blocks at the southeast end of a major shear-fracture zone (January-Norton) against major north-south offsets. The location of the main manto orebody itself is due to favorable host rocks and the permeability contrast created by the slightly earlier but cogenetic jasperoid caprock.

ACKNOWLEDGEMENTS

This study has been financed by ASARCO Incorporated which generously gave permission for the original field trip and this publication. S. R. Davis, F. T. Graybeal, and P. G. Vikre were particularly helpful critics of this work. The majority of the surface mapping, division of stratigraphic units, and initial drill logs are the excellent work of S. R. Davis. Many others at Asarco, particularly A. Dalla Vista and N. P. Whaley, have contributed to this study over the years.

This study is part of Ph.D. work at the Department of Geosciences, University of Arizona, directed by S. R. Titley. Professor Titley and a large number of students who have helped this study by assisting in the field and laboratory and providing a sounding-board for ideas deserve many thanks.

N. E. Lehman, T. L. Heidrick, J. J. Quinlan, and J. Wilkins are thanked for their help with the original field trip.

SELECTED REFERENCES

Baker, R. C., 1961, The Geology and Ore Deposits of the Southeastern Portion of the Pagatonia Mountains, Santa Cruz County, Arizona: Ph.D. Thesis, Univ. Michigan, 287 p.

Burns, R. G. and Burns, V. M., 1977, "Mineralogy" in: Glasby, G. P. (ed), Marine Manganese Deposits, Chap. 7, p. 185-248, Elsevier Oceanographic Series, Vol. 15.

Davis, S. R., 1970, Hardshell Geological Report, Harshaw Mining District, Santa Cruz County, Arizona: ASARCO internal report.

Kartchner, W. E., 1944, The Geology and Ore Deposits of a Portion of the Harshaw District, Patagonia Mountains, Arizona: Ph.D. Dissertation, Univ. Arizona.

Keith, S. B., 1975, Index of Mining Properties in Santa Cruz County, Arizona: Ariz. Bur. Mines Bull. 191, 94 p.

Koutz, F. R., 1977, Silver, Base-metal Manganese Oxides and Fluid Inclusion Geothermometry, Hardshell Manto, Patagonia Mountains, Arizona: Geol. Soc. Amer., Abstr. with Prog. v 9, n 7, p. 1056-57.

Moores, R. C., 1972, The Geology and Ore Deposits of a Portion of the Harshaw District, Santa Cruz County, Arizona: M.S. Thesis, Univ. Arizona, 98 p.

Simons, F. S., 1972, Mesozoic Stratigraphy of the Patagonia Mountains and Adjoining Areas, Santa Cruz County, Arizona: U. S. Geol. Surv. Prof. Paper 658E, 23 p.

Simons, F. S., 1974, Geologic Map and Sections of the Nogales and Lochiel Quadrangles, Santa Cruz County, Arizona: U. S. Geol. Surv. Map I-762, 1:48000 and 9 p. explanation.

Simons, F. S., Raup, R. B., Hayes, P. T., Drews, H., 1966, Exotic Blocks and Coarse Breccias in Mesozoic Volcanic Rocks of Southeastern Arizona: U. S. Geol. Surv. Prof. Paper 550-D, p. 12-22.

Schrader, F. C., 1915, Mineral Deposits of the Santa Rita and Patagonia Mountains, Arizona, with contribution by J. M. Hill: U. S. Geol. Surv. Bull. 552, 373 p.